Journal of Iberian Geology (2024) 50:137–156
https://doi.org/10.1007/s41513-024-00236-y

RESEARCH PAPER

Inorganic geochemistry of Miocene sediments from the Lower Chelif Basin (NW Algeria) for approaching weathering and palaeoclimatic conditions

Fatiha Hadji[1] · Abbas Marok[1] · Ali Mokhtar Samet[2] · Matías Reolid[3] · Kamar Eddine Bensefia[1]

Received: 15 October 2022 / Accepted: 7 April 2024 / Published online: 29 April 2024

Abstract

Geochemical studies of major and trace elements were conducted on Miocene sediments from three sections of the Lower Chelif Basin, Northern Algeria. Geochemical proxy records demonstrate that the Lower Chelif Basin has experienced weak to moderate weathering and the Index of Compositional Variability (ICV) values suggest that these sediments were, in general, enriched in rocks forming minerals. Al_2O_3 *versus* (*vs.*) K_2O diagrams indicate that, in Miocene sediments, the minerals containing Al_2O_3 and K_2O are primarily illite; likely derived from K-feldspar decomposition. The application of the Al_2O_3 *vs* TiO_2 binary plot, as a provenance indicator, indicates that all the samples fall along the basalt + rhyolite/granite line indicating that the sediments derived from mixed source sediments the composition of which ranges from mafic and felsic rocks. Compared to Upper Continental Crust (UCC) composition, Miocene sediments depict strong depletion in SiO_2, Al_2O_3, MnO, Na_2O, K_2O, Zr and Sr during the weathering process as well as an enrichment in Cr and Cu. Calculated percentage variation plotted against the Chemical Index of Alteration (CIA) diagrams provides a basis for assessing the chemical mobility during weathering in the Chelif Basin. For the study stratigraphical range, Si, Al, Mn, Na and K show depletion in relation to Ti. Sodium decreases more rapidly than K, suggesting a Na-plagioclase alteration higher than that of K-feldspar. During the Tortonian, the chemical motilities of Rb and K are tightly correlated ($r = 0.72$), but the former decreases lesser. Calculated values of C-proxy suggest a roughly semi-arid to semi-moist climate during the Burdigalian-Langhian, arid to semi-arid during the Tortonian and more humid conditions during the Messinian. Sr/Ba ratio ranging from 0.44 to 6.48 indicates a palaeoenvironment with variable salinity during the Miocene.

Keywords Chelif Basin · Northern Algeria · Miocene · Geochemistry · Weathering · Provenance

✉ Abbas Marok
a_marok@yahoo.fr

Fatiha Hadji
fm_hachemi@yahoo.fr

Ali Mokhtar Samet
mokhtarsametali@yahoo.fr

Matías Reolid
mreolid@ujaen.es

Kamar Eddine Bensefia
bkamareddine@yahoo.fr

[1] Department of Earth and Universe Sciences, University of Tlemcen, P.O. Box 119, Tlemcen, Algeria

[2] Department of Hydraulics, University of Chlef, P.O. Box 151, Chlef, Algeria

[3] Departamento de Geología, Universidad de Jaén, Campus Las Lagunillas S/N, 23071 Jaén, Spain

Resumen
Se han llevado a cabo los análisis químicos de elementos mayoritarios y traza de los sedimentos miocenos de tres secciones estratigráficas de la Cuenca del Bajo Chelif en el Norte de Argelia. El registro de indicadores geoquímicos demuestra que la Cuenca del Bajo Chelif ha experimentado una meteorización entre débil y moderada y los valores del Índice de Variación Composicional sugieren que estos sedimentos estaban, en general, enriquecidos en minerales petrogenéticos. Los diagramas Al2O3 vs. K2O muestran que, durante el Mioceno, el principal mineral que contiene Al3+ y K+ fue la ilita, probablemente originada por alteración de feldespato potásico. La aplicación del diagrama Al2O3 vs TiO2, como indicador de procedencia apunta a que todas las muestras caen en la línea que separa los campos de basalto y riolita/granito, lo que indica que el sedimento deriva de una fuente mixta con una composición que varía entre una fuente de rocas máficas y félsicas. Comparado con la composición promedio de la corteza continental superior (UCC), los sedimentos miocenos muestran un fuerte empobrecimiento en SiO2, Al2O3, MnO, Na2O, K2O, Zr y Sr producido durante la meteorización así como un enriquecimiento en Cr y Cu. Los diagramas de porcentaje de variación de los distintos elementos respecto a la UCC frente al índice de alteración química (CIA) proporcionan la base para comprender la movilidad química durante la meteorización en la Cuenca del Chelif. Para el intervalo estratigráfico estudiado el Si, Al, Mn, Nay K muestran empobecimiento respecto al Ti. El Na decrece más rápidamente que el K, sugiriendo una mayor alteración de la plagioclasa sódica que del feldespato potásico. Para el Tortoniense, la movilidad de Rb y K está claramente relacionada (r = 0.72), con una menor disminución del Rb. Los valores del índice-C (C-proxy) sugieren un ambiente entre semiárido y semihúmedo durante el Burdigaliense-Langiense, entre árido y semiárido para el Tortoniense y más húmedo durante el Messiniense. La relación Sr/Ba, que varía entre 0.44 y 6.48, indica un paleoambiente con variable salinidad durante el Mioceno.

Palabras clave Cuenca de Chelif · Norte de Argelia · Mioceno · Geoquímica · Meteorización · Procedencia

1 Introduction

Geochemistry of sedimentary rocks provides important information about the provenance and environmental conditions in the sedimentary basin. Analyzing the composition of elements in rocks or sediments (both major and trace elements) is a valuable method for evaluating the extent of chemical weathering and for understanding the geological processes that have affected them (Liu et al., 2009; Nesbitt & Young, 1982; Singh et al., 2005). Approaches can be carried out by a great variety of methods discussed in literature such as indexes of chemical weathering (e.g. Fedo et al., 1995; Harnois, 1988; Nesbitt & Young, 1982; Parker, 1970), ratios and bivariate plots to decipher provenance (e.g. Amajor, 1987; Hayashi et al., 1997) and calculated ratios for determining climate and salinity conditions (Jian et al., 2012; Meng et al., 2012; Vosoughi Moradi et al., 2016).

In Northern Algeria, geological researches conducted on the Miocene successions of Lower Chelif Basin are mainly focused on biostratigraphical, palaeogeographical and geodynamic aspects (e.g. Belkebir, 1986; Belkebir et al., 1996; Belkebir et al., 2002; Bessedik et al., 2002; Belhadji et al., 2008). To our knowledge, very few researches have focused on geochemical analyses aiming at a reconstruction of palaeoenvironmental conditions. This work is focused on the geochemical analysis of the Miocene rocks from three reference sections selected from the northern and southern margins of the Lower Chelif Basin. The aim of this study is to decipher the degree of palaeo-weathering, the provenance, and the palaeoclimate and palaeosalinity of the depositional conditions during different intervals of Miocene: Burdigalian-Langhian, early Tortonian, and early Messinian.

2 Geological setting and stratigraphic framework

After the 80's, many pluridisciplinary works have been made on the Lower Chelif Basin (Meghraoui, 1982, 1986; Rouchy, 1982; Rouchy, et al., 2007; Thomas, 1985; Belkebir, 1986; Ameur-Chehbeur, 1988; Saint-Martin, 1990; Neurdin-Trescartes, 1992, 1995; Belkebir et al., 1996; Belkebir et al., 2002; Bessedik et al., 2002; Aifa et al., 2003; Atif et al., 2008; Belhadji et al., 2008; Mansour et al., 2008; Arab et al., 2015). This 100 -km-long synorogenic basin belongs to the sublittoral Neogen basins of northwestern Algeria. It is located between the littoral massifs (Murdjadjo, Orousse and Dahra) to the North, and the Tessala Mountains, Ouled Ali, Béni Chougrane and Ouarsenis, to the South (Fig. 1A). The Lower Chelif Basin is related to paroxysmal phases of the Alpine Orogen (e.g. Aïfa et al., 1992; Arab et al., 2015; Neurdin-Trescartes, 1992; Thomas, 1985; Wildi, 1983) and is characterized by Miocene to Quaternary sediments overlying unconformably Mesozoic basement (Cretaceous schists)

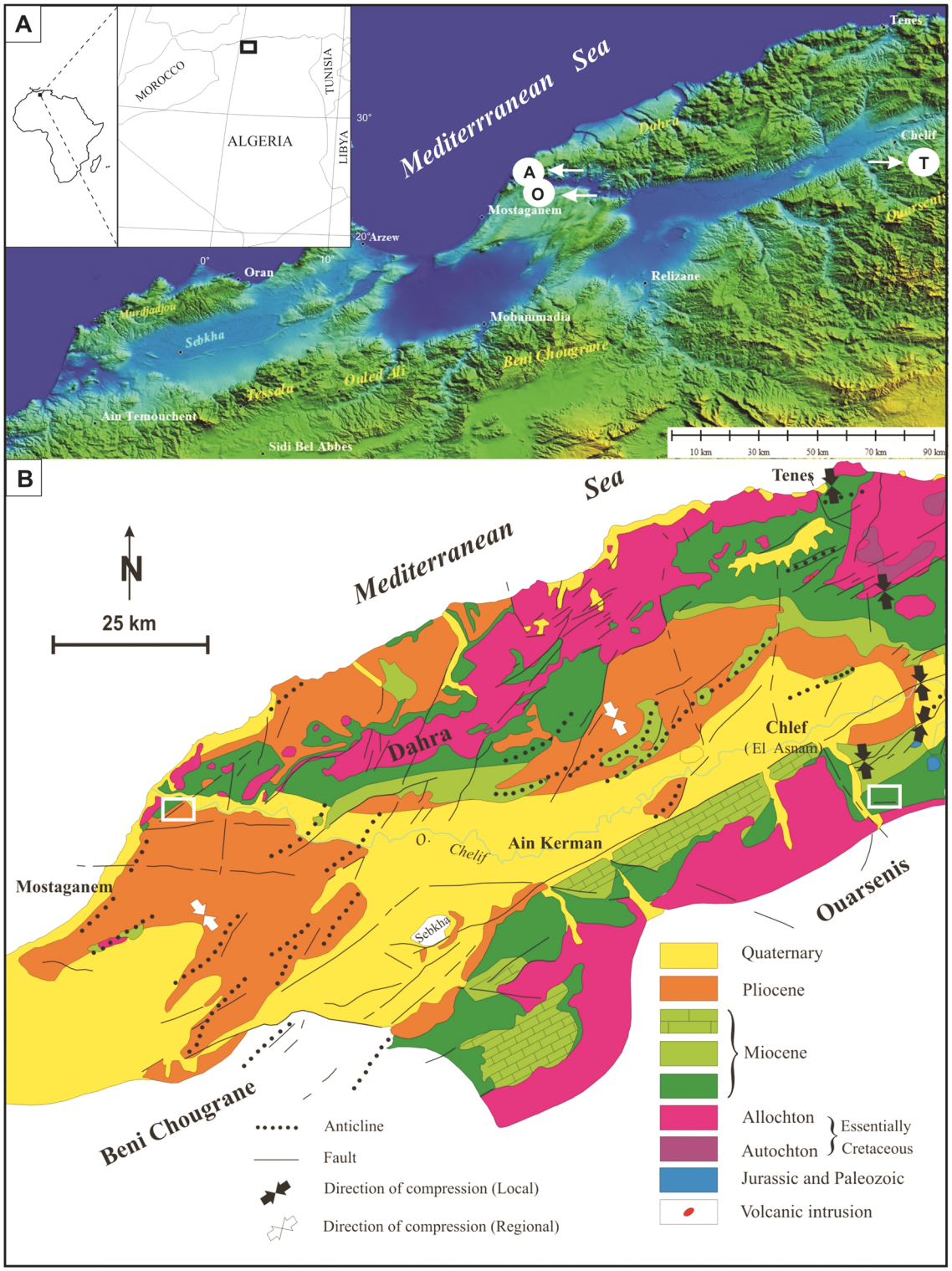

Fig. 1 Geographic and geological sketch. **A** Map of the Chelif Basin trough the Miocene with location of the studied section (modified from Rouchy et al., 2007). **B** Geological and tectonic map of the Lower Chelif Basin (from Meghraoui, 1986)

(Fig. 1B). In this area, the occurrence of alkaline and calc-alkaline rock types was reported by Aifa et al. (1992).

The rock layers of the lower Miocene, along with their corresponding features, display notable variations that manifest in both geographically and stratigraphically. These distinctions are evident across diverse locations within a given area, showcasing spatial heterogeneity. Moreover, the characteristics of these lower Miocene rocks undergo changes at different points in geological history, highlighting temporal dynamics. This variability underscores the complexity and dynamic nature of the lower Miocene geological formations.

Therefore, the mostly marine sediments are mainly composed of bluish marls that laterally change into sandstones, purple indurated marls and conglomerates (e.g. Bessedik et al., 2002). According to Neurdin-Trescartes (1992, 1995) and Arab et al. (2015), the marine lower Miocene was deposited during a compressional episode in a piggyback position on top of the still moving Tellian allochthonous block.

The middle Miocene marine deposits consist of conglomerates, sandstones and blue to grey marls attributed to the Langhian (Belkebir et al., 1996). This succession is overlain by the Serravallian grey marls, sandstones, red clays and conglomerates (Bessedik et al., 2002).

During the late Miocene (Tortonian-Messinian), the North- and Southern margins of the Chelif Basin were characterized by sedimentation from marine and continental environments (blue marls, diatomites and evaporites) showing a significant variation in thickness.

The Ouillis and Amarna sections from the northern margin of the Lower Chelif Basin, and the Tiraouet section from the southern margin are the three sections have been discussed in this study (Fig. 1A).

3 Stratigraphic setting of the studied sections

3.1 Tiraouet section

The Tiraouet section, is located in the SE of Chlef village, around 15 km North from Sendjas (Fig. 1). This section consists of marls assigned to uppermost Burdigalian–Langhian by Bessedik et al.(2002)(Fig. 1). The association of planktic foraminifera is represented by the *Globigerinoides trilobus* and *Globoquadrina baroemoensis* species which confirm the Burdigalian-Langhian age attributed by Bessedik et al. (2002). The studied section is 73-m thick (Figs. 2 and 3) and is made of:

- -Blue marls (39 m) passing to sandy marls to the top. This stratigraphic interval is topped by a 0.8-m thick cineritic bed (Fig. 3).
- -Purple indurated marls (34 m) devoid of macroinvertebrate fossils, overlain by a conglomerate bar.

3.2 Ouillis section

This basin northern margin section is located in the southwestern part of the Dahra Massif, to the North of Sidi Bel Attar locality (Fig. 1). Samples were collected at the Ouillis Quarry, where this section consists of the upper part of the diatomitic formation (19 m). This stratigraphic interval can be subdivided into two distinct lithological units as shown in Fig. 2:

3.2.1 Member A

This member (14 m) is represented by centimetric to decimetric marl/diatomite alternation. From bottom to top are distinguished (Mokhtar Sametet al. 2022; Fig. 3):

- Nine meters of monotonous alternation of marls and white diatomite beds, starting with a 10 cm-cineritic level. The beige base and top of the diatomitic beds are more or less marly, passing gradually into marly terms. Massive and platelet-form marly intervals (0.15–0.70 m) are brown at the base, becoming black and passing gradually to diatomite facies. Samples collected from this section have delivered radiolarian associations with *Dictyocoryne* sp., *Hymeniastrum* sp., *Actinosphaera* sp., *Ctinosphaera* sp. and *Porodiscus* sp. (Mokhtar Samet et al. 2021, 2022).
- Five meters of tight alternation of 11 sequences including laminated diatomite-marls and laminated diatomite-marls-gypsum terms. Gray laminated diatomites contain sometimes fish scales and black marl (0.10–0.70 m), showing occasionally lamination. The presence of five 1–2 cm-thick gypsum levels was distinguished.

3.2.2 Member B

This member (5 m) is characterized by a rhythmic alternation of marls and diatomite beds (Fig. 3). The vertical organization of this member shows the presence of three binary sequences (marl-diatomite). To the top the grayish/beige marls reveal the presence of intercalations of three-centimeter thick beds of diatomites. This member ends with

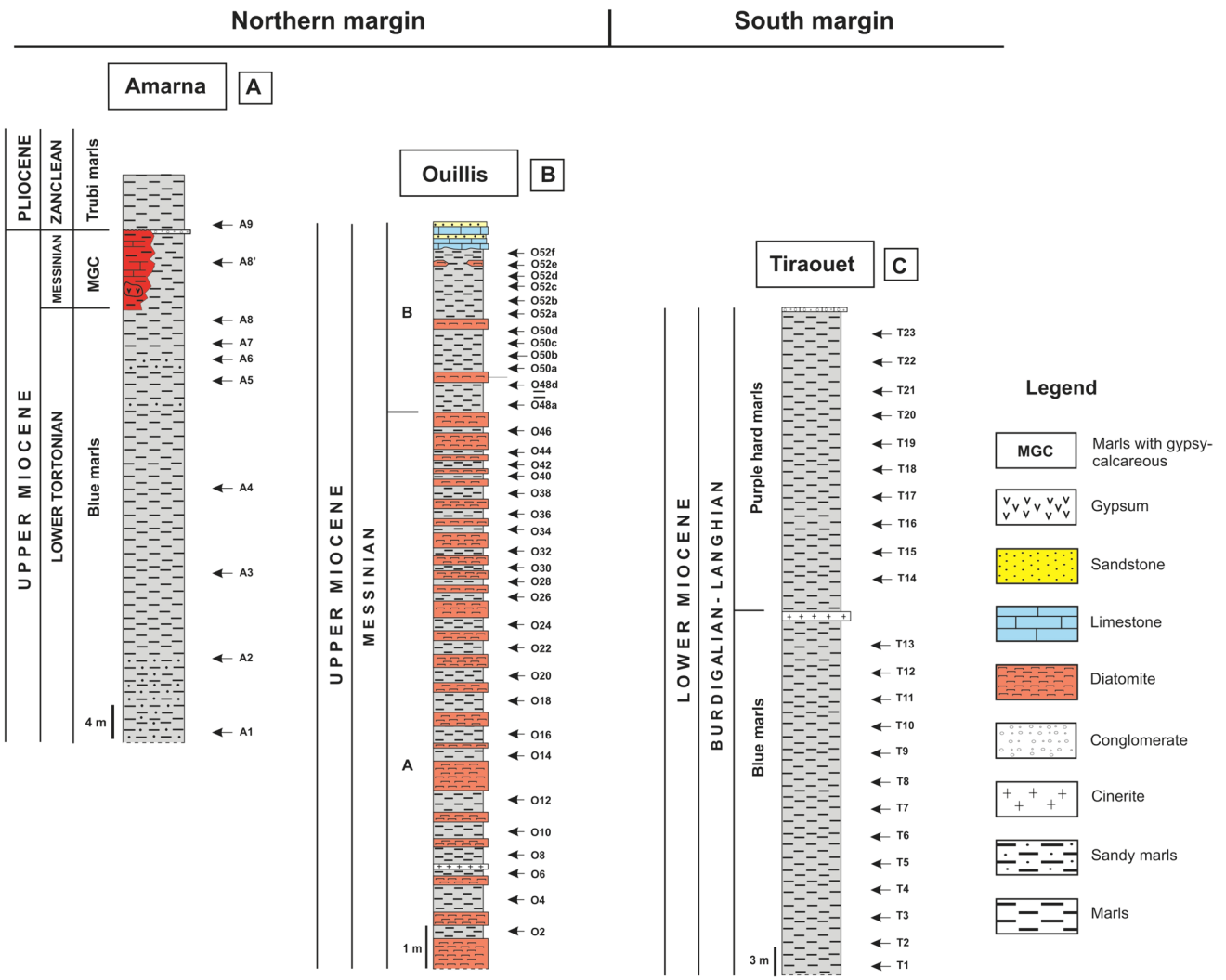

Fig. 2 Stratigraphic column of **A** Amarna, **B** Ouills and **C** Tiraouet sections

centimetric limestone beds resting on the underlying marls via gullies.

In the Ouillis section, the diatomitic formation age determination was based on micropaleontological data and regional correlations (Mokhtar Samet et al. 2021, 2022). In fact, a single association of benthic foraminifera characterizes the member B of the study section, including: *Bulimina subulata, Bulimina aculeata, Bolivina dilatata, Bolivina dentellata, Uvigerina* sp. and *Rectuvigerina cylindrica*. This association allows to assign a Messinian age (*Globorotalia mediterranea* Biozone). Regional correlations and diatom assemblages of the member A from the area (Bois Sacré, Douar Ouled Bettahar and Djebel Ben Dourda sections) allowed to Mansour et al. (2008) to confirm the attributed Messinian age (upper Miocene).

3.3 Amarna section

Amarna section is located to the northeastern of Djebel Diss (northern margin of the Chelif Basin), about 16 km North from Mostaganem city (Fig. 1). This section is composed of three formations (Fig. 2):

- -*Blue marls* Fm (64 m): yellowish sandy marls at the base and blue marls to the top (Fig. 3).This unit is covered by a 0.30 m-thick conglomerate bar. The planktic foraminifera association consists mainly in *Neogloboquadrina acostaensis*, *Globorotalia scitula*, *Globigerinoides obliquus*, *Globigerinoides trilobus*, *Globigerina bulloides*. This enabled us to give a lower Tortonian age (*Neogloboquadrina acostaensis* Biozone) to this member and confirms the datation of Belhadji et al. (2008).

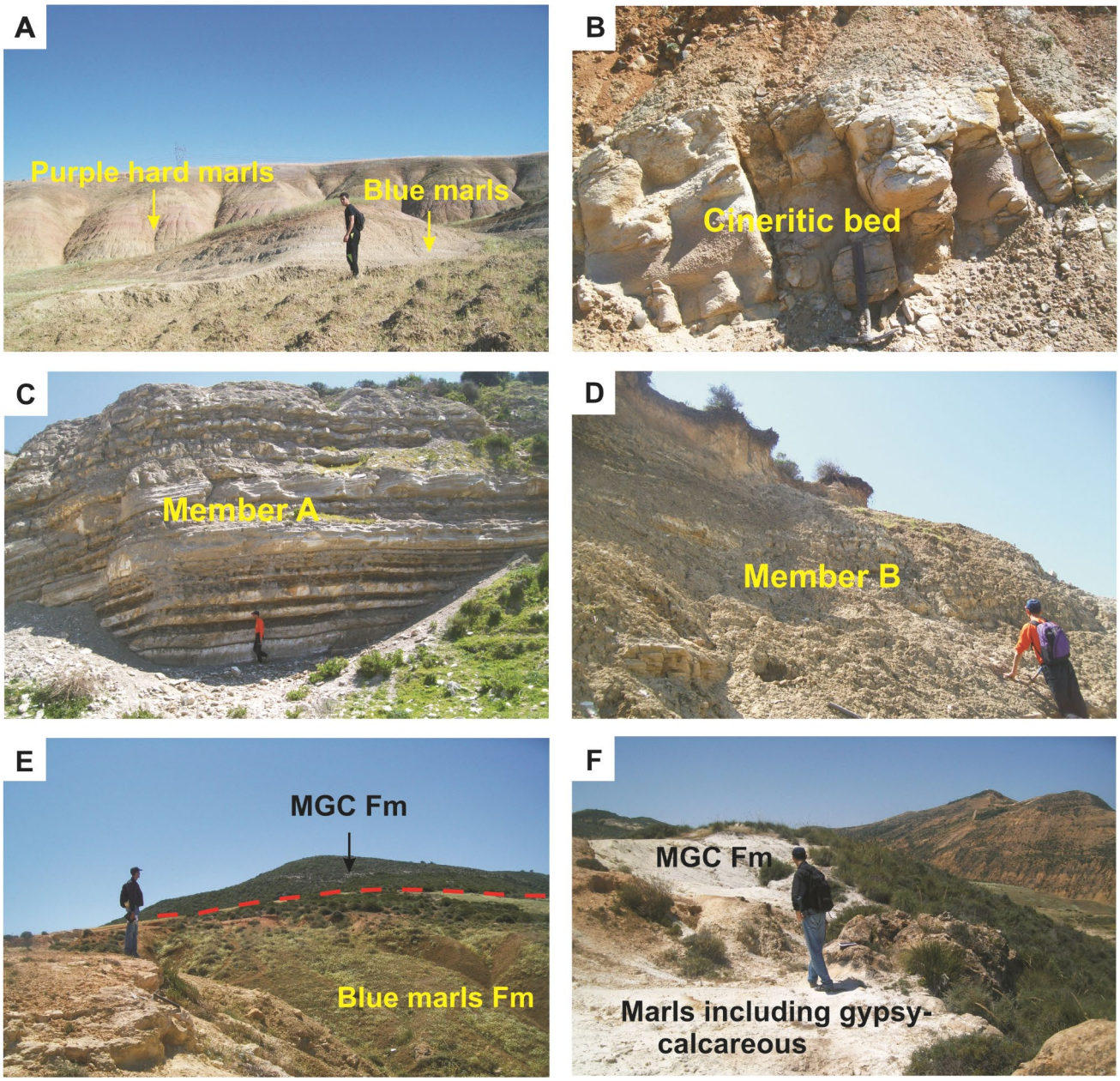

Fig. 3 Photographs of the Miocene formations

- *-Marls with gypsum-limestone intercalations* (MGC Fm) (10 m): this marl outlier formation includes gypsum-limestone beds (Fig. 3F). It has been dated as upper Messinian by correlation with the Mediterranean Basin evaporite deposits (Belhadji et al., 2008). This mainly evaporitic succession is overlain by the Pliocene (Zanclean) Trubi Fm whitish marls.

4 Proxies for chemical mobility and enrichment and palaeoclimate

4.1 Proxies for chemical mobility and enrichment

Weathering is primarily a function of the mobilization, fractionation and redistribution of major and trace elements (Singh et al., 2005). It is affected by various processes such as dissolution, hydration, and oxidation of primary minerals, and formation of secondary minerals, transportation of material, and ion exchange

on various minerals (Chesworth et al., 1981; Nesbitt et al., 1980). Titanium is relatively immobile during weathering (Nesbitt, 1979) and is consequently chosen for the calculation of chemical mobility of major and trace elements (Hill et al., 2000; Middleburg et al., 1988; Singh et al., 2005). Percentage change of major and trace elements were evaluated in terms of percentage shifts of each element. The enrichment factor EF for any element x is given by the following equation:

$$EF(\%) = \frac{(X/TiO_2)Sample}{(X/TiO_2)UCC}$$

4.2 Proxies for palaeoclimate

It is generally accepted that Fe, Mn, Cr, V, Ni and Co are relatively enriched under moist conditions (Jian et al., 2012). In contrast, the strengthening of water alkalinity due to evaporation under arid conditions causes saline minerals precipitation, leading Ca, Mg, K, Na, Sr and Ba to concentrate (Jian et al., 2012). Considering the different chemical behavior and nature of the both above defined groups of elements, their ratio is proposed as a proxy for climatic change. In this context, Zhao et al. (2007), Cao et al., (2015) and Vosoughi Moradi et al. (2016) applied de C-value [C-value = (Fe + Mn + Cr + Ni + V + Co)/(Ca + Mg + Sr + Ba + K + Na)] as an indicator for palaeoclimate.

5 Material and methods

This research is based on the processing and analysis of 48 marl samples from the Tiraouet (23), Ouillis (17) and Amarna (8) sections (Fig. 2). Total elements contents were analyzed at Tlemcen University using a sequential XRF spectrometer (Wavelength- Dispersive, Brucker-Axs: SRS 3400) on homogenized powdered bulk samples. Samples, reduced to powder, were mixed with lithium tetraborate, and then melted at 1200 °C to obtain transparent and homogeneous glasses (borate beads). When the samples are not suitable for this process, they are prepared in the form of pellets. An analysis program was established based on the type of sample and concentration range, including the chemical elements to be quantified. The obtained borate beads or pellets were subjected to primary X-ray radiation source, which leads to the excitation of atoms that will emit a characteristic secondary X-ray fluorescence radiation indicative of the chemical composition of the sample being analysed. Data processing was performed using the Spectra 3000AT software. The main elements analyzed as weight percentage of oxides were SiO_2, Al_2O_3, Fe_2O_3, CaO, MgO, Na_2O, K_2O,

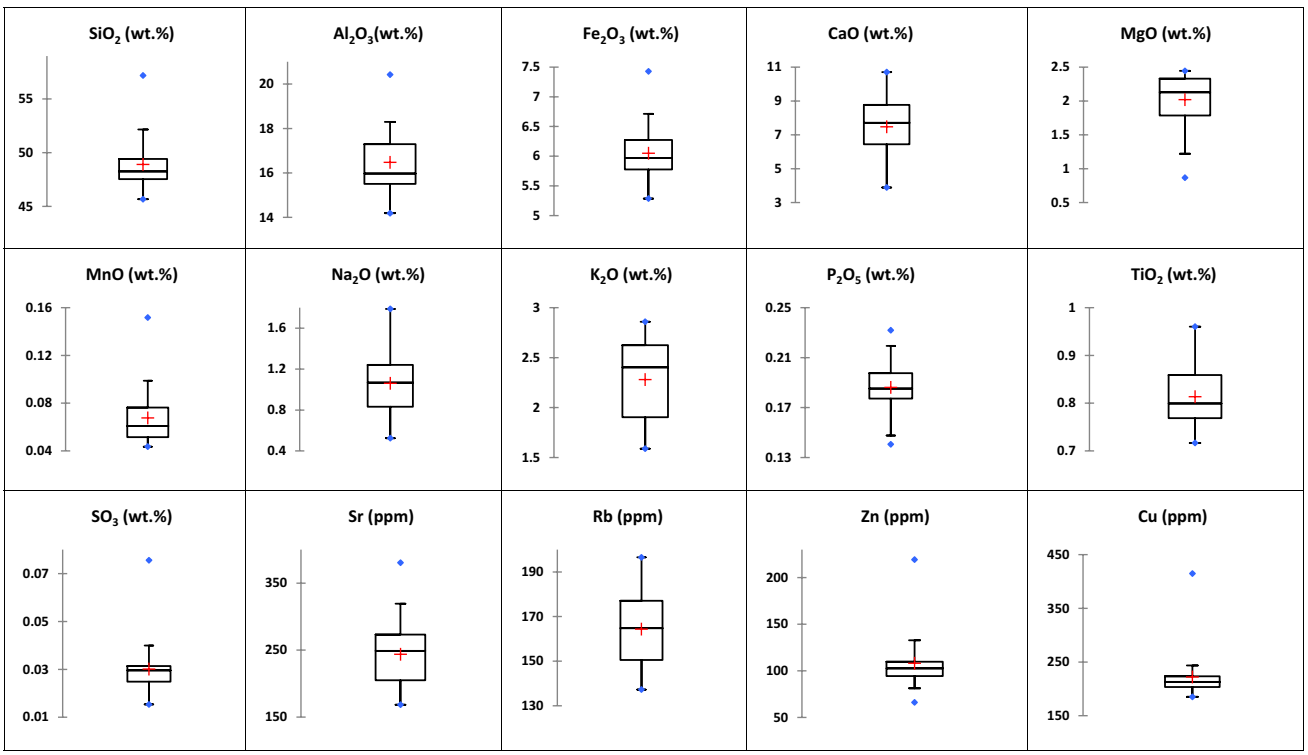

Fig. 4 Box plots of Tiraouet sample sediments

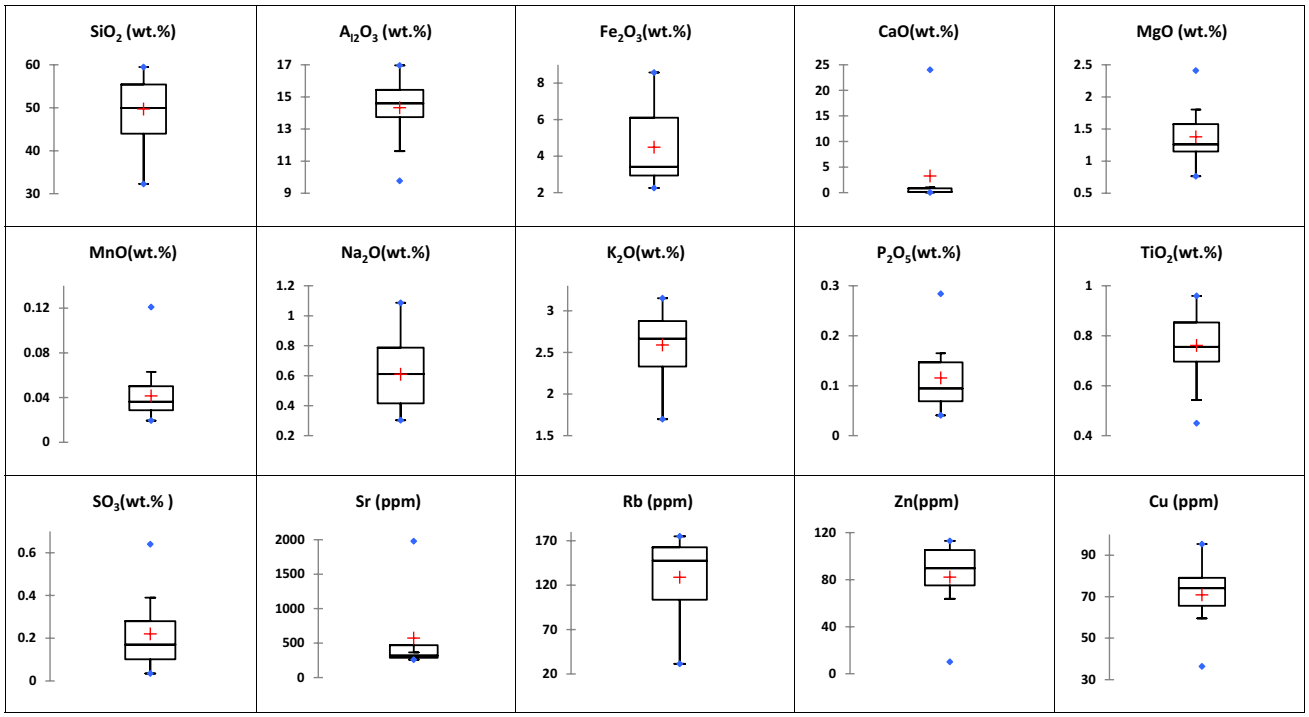

Fig. 5 Box plots of Amarna sample sediments

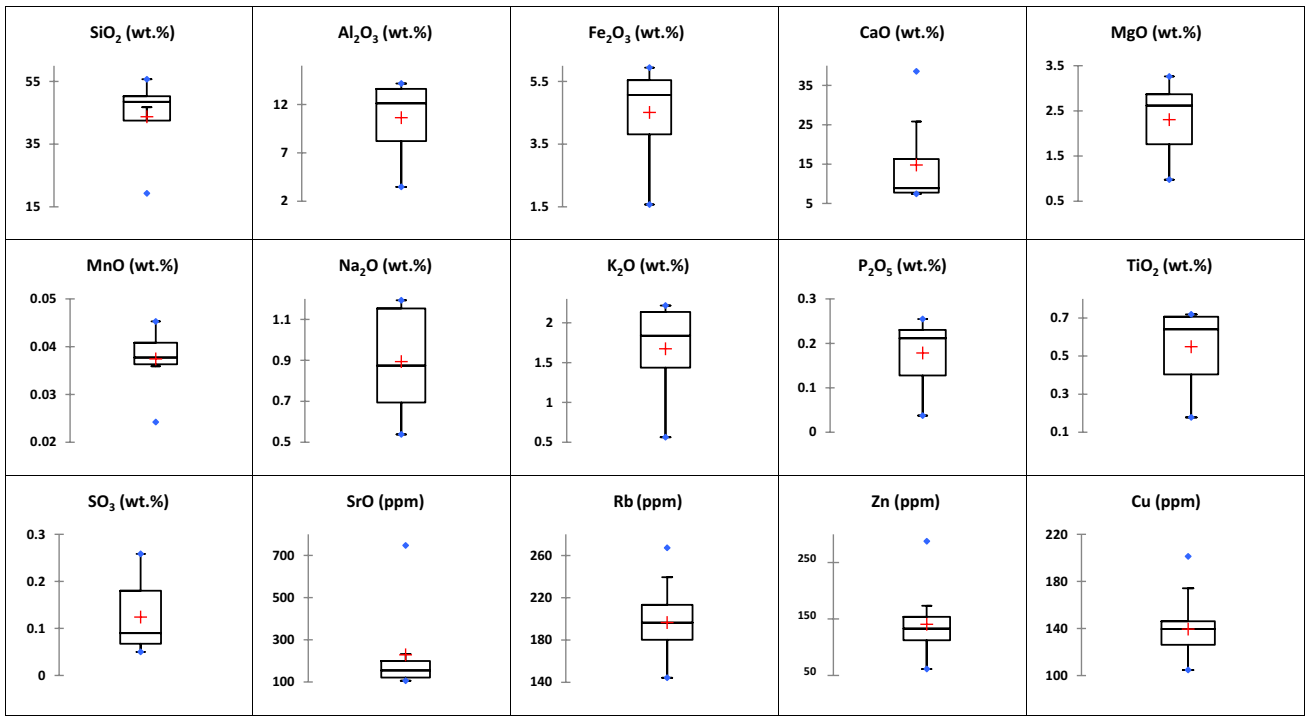

Fig. 6 Box plots of Ouillis sample sediments

P_2O_5, SO_3, MnO, and TiO_2. Trace elements contens (Rb, Sr, Ba, Ni, Cr, Cu, Zr, Zn, and Pb) are expressed as parts per million (ppm). The concentrations of oxides and trace elements of the analyzed samples are reported are reported in Figs. 4, 5, 6.

The degree of chemical weathering for the Miocene sediments was calculated using the Chemical Index of Alteration (CIA) (Nesbitt & Young, 1982) and Plagioclase Index of Alteration (PIA) (Fedo et al., 1995). These indexes can be used for quantitative evaluation of the weathering degree of rocks. The used formula for CIA is given by: $CIA = 100 \times Al_2O_3/(Al_2O_3 + CaO^* + Na_2O + K_2O)$ where CIA is a non-dimensional parameter ranging from 0 to 100, corresponding to increasing weathering and sediment maturity. Element abundances are expressed as molar proportions and CaO* represents the Ca associated within the silicate mineral/non-carbonate fraction of the sediment. The CaO* concentrations were calculated using the formula by Fedo et al. (1995).

The PIA provides a quantitative estimation of secondary clay mineral from primary feldspars (Nesbitt & Young, 1982) and volcanic glasses (Fedo et al., 1995). During the weathering of feldspar from the source rock, Ca is considerably leached quickly in comparison to Na and K. Therefore, with an increasing intensity of weathering, the total alkali content in the rock and K_2O/Na_2O ratio are of opposite variations (a decrease in total alkali $K_2O + Na_2O$ content is related to an increase in K_2O/Na_2O ratio). It is considered as being due to the fact that the breaking down and removal of plagioclase feldspar is rather preferred instead of K-feldspars (Nesbitt & Young, 1984). For fresh rocks, PIA is 50; however, for some clay minerals (kaolinite, illite, smectite), it is approximately 100 (Fedo et al., 1995).

The Index of Compositional Variability (ICV) of Cox et al. (1995) given by $ICV = (Fe_2O_3 + K_2O + Na_2O + CaO + MgO + MnO + TiO_2)/Al_2O_3$, is a proxy for indicating the maturity degree of alumino-siliciclastic materials delivered to the sedimentary basin (Maslov et al., 2003). Immature shales with a high percentage of silicate minerals (except clay minerals) are characterized by ICV > 1. In contrast, more mature clayey rocks with abundant proper clay minerals have lower ICV values (Maslov et al., 2003). Values of ICV < 1 are typical of minerals such as illite, kaolinite, and muscovite; higher values (> 1) being characteristic of rock forming minerals such as plagioclase, K-feldspar, amphiboles and pyroxenes (Cox et al., 1995; Moosavirad et al., 2011).

The SiO_2/Al_2O_3 ratio is a significant index for indicating the maturity of sedimentary rocks and the K_2O/Al_2O_3 ratio is commonly used as an indicator of the original composition of sediments. The K_2O/Al_2O_3 ratio can evaluate the amount of alkali feldspar vs. plagioclase and clay minerals within the original shales (Cox et al., 1995). According to these authors, this ratio is < 0.3 for clays but ranges between 0.3 and 0.9 for feldspar. Sediments with K_2O/Al_2O_3 ratios > 0.5 suggest a relatively significant amount of alkali feldspar within the original shale; those < 0.4 indicate a minimal alkali feldspar in the original shale (Cox et al., 1995).

Al_2O_3/TiO_2 ratios of most clastic rocks are essentially used to infer the source rock compositions. In fact, this ratio increases from 3 to 8 for mafic igneous rocks, from 8 to 21 for intermediate rocks, and from 21 to 70 for felsic igneous rocks (Hayashi et al., 1997).

We have also applied the geochemical proxy C-value [C-value = (Fe + Mn + Cr + Ni + V + Co)/(Ca+Mg+Sr+Ba+K+Na)] as an indicator for palaeoclimate (Zhao et al., 2007; Cao et al., 2015; Vosoughi Moradi et al., 2016). This geochemical proxy relates elements typically enriched under moist conditions (Fe, Mn, Cr, V, Ni and Co; Jian et al., 2012) and elements relatively enriched under arid conditions (Ca, Mg, K, Na, Sr and Ba; Jian et al., 2012).

The Zr/Al and Rb/Al are used as detrital proxies of eolian contribution (Zr/Al; Pye, 1987; Rodríguez-Tovar & Reolid, 2013) and fluvial transport (Rb/Al; Chester et al., 1977; Mokhtar Samet et al., 2022; Rodríguez-Tovar & Reolid, 2013).

6 Results

6.1 Major oxides and trace elements

In the lower Miocene sediments of the Tiraouet section, major oxide contents consist of 45.68 to 57.19% SiO_2; 14.31 to 20.42% Al_2O_3; 5.29 to 7.43% Fe_2O_3; 3.89 to10.70% CaO (Fig. 4). Within the spectrum of analyzed trace elements, particular significance is attributed to the content variations of three key elements. Strontium demonstrates noteworthy concentrations, spanning from 168 to 381 ppm, Cu exhibits a range of concentrations extending from 185 to 415 ppm, and Ba displays considerable variability, with content levels ranging between 70 and 476 ppm (Fig. 4).

Within Tortonian sediments of Amarna section, contents ofSiO_2 (19.30 to 51.54%); Al_2O_3 (3.48 to 13.94%), Fe_2O_3 (1.57 to 5.94%) and CaO (7.46 to 38.58%) are generally lower than that of the lower Miocene of Tiraouet section (Fig. 5). Among the analyzed trace elements, Sr presents the highest concentration (260 to 1978 ppm) followed by Ba (196 to 396 ppm) (Fig. 5).

In the case of the lower Messinian sediments of the Ouilis section, main elements consist of SiO_2 (32.28 to 59.49%), Al_2O_3 (9.77 to 16.97%) and CaO (0.03 to 24.04%) (Fig. 6). Among the analyzed trace elements, highest contents correspond to Ba (317 to 3822 ppm), Sr (106 to 748 ppm) and Rb (144 to 267 ppm)(Fig. 6).

6.2 Chemical proxies for weathering and maturity

According to Song et al., (2014), CIA values in the intervals of 50–65, 65–85 and 85–100 represent, respectively, weak weathering under cold and dry climatic

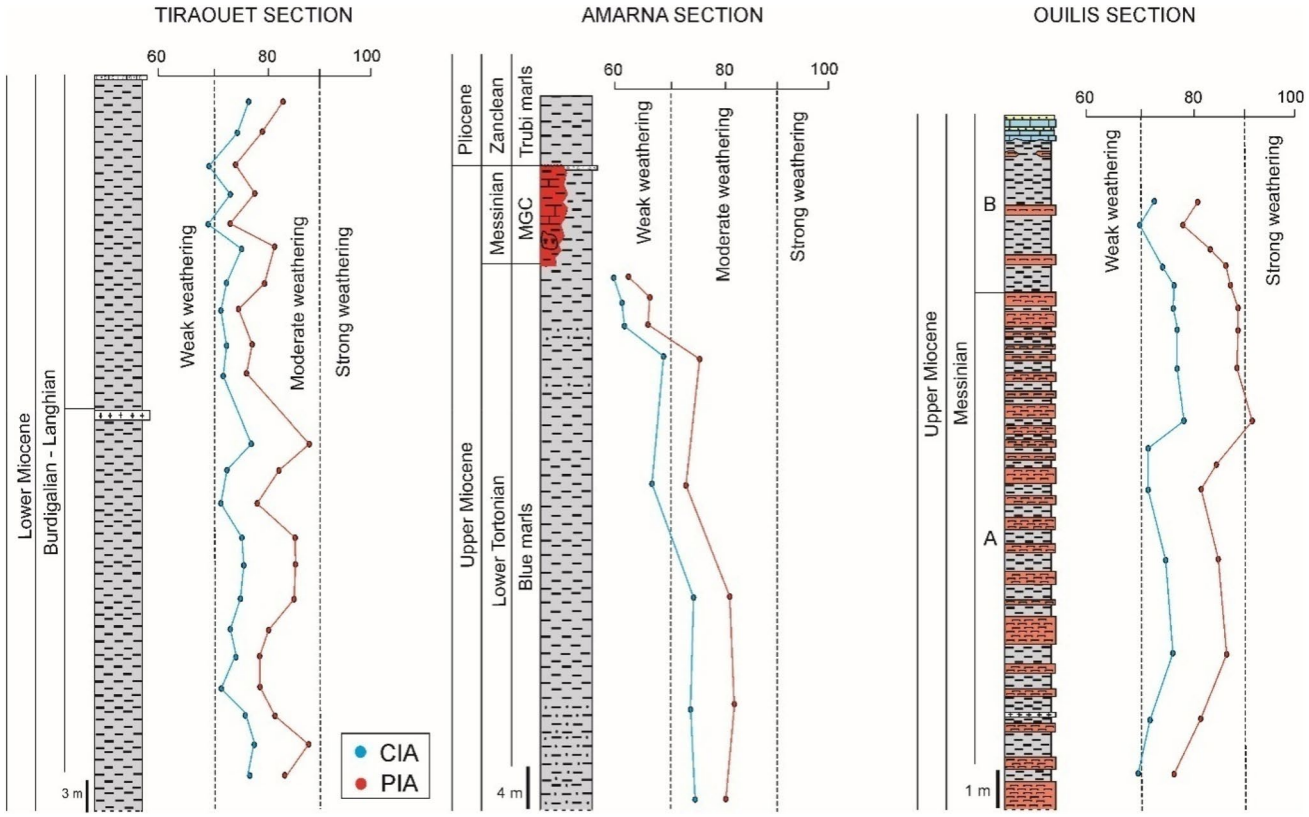

Fig. 7 Vertical variations of CIA and PIA of Tiaouret, Amarna and Ouillis sections

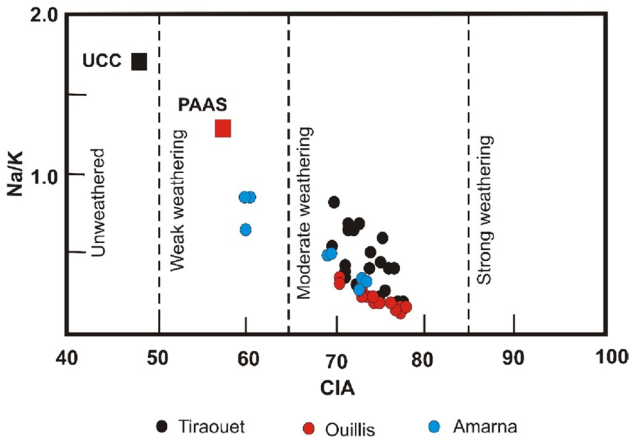

Fig. 8 Scatter diagram of CIA vs. Na/K molar ratio of Miocene sediments. Chemical composition of and PAAS after McLennan (2001) and UCC after Rudick and Gao (2003)

conditions, moderate weathering under warm and moist conditions, and strong chemical weathering in tropical or subtropical areas under hot and humid conditions.

The CIA values of the lower Miocene in the Tiraouet section vary between 68.69 and 76.79 (average 73.56, standard deviation (SD) 2.35). Those of the Tortonian sediments, in Amarna section, range from 59.41 (top) to 74.72 (average 67.78, SD 6.74) which indicates that these rocks experienced a weak to moderate weathering. CIA values of Messinian sediments in Ouillis section vary between 70.02 and 79.25 (average 74.98, SD 2.65) (Fig. 7).

These values are higher than that admitted for the upper continental crust (UCC) without weathering (CIA = 48, Rudnick & Gao, 2003) and post-Archean Australian Shale (PAAS, CIA = 70, Taylor & McLennan, 1985; and CIA = 57, McLennan, 2001), implying that all Miocene sedimentary rocks have suffered from weak to moderate weathering (Fig. 7).

The sediments from the three stratigraphic intervals studied are clearly differentiated from a scatter diagram of CIA vs. Na/K ratio (Fig. 8). Lower Messinian samples from Ouillis section are clearly characterized by the lowest values of Na/K ratio. The lower Tortonian samples from Amarna section present the lowest values of CIA.

In the present study, PIA values are variable in the different sections. For Lower Miocene sediments of the Tiraouet section they range from 73.34 to 87.97 (average 80.45; SD 4.05). PIA values are relatively lower in the lower Tortonian of Amarna section ranging from 61.88 to 83.10 (average 73.27; SD 9.10), with a decreasing trend to the top

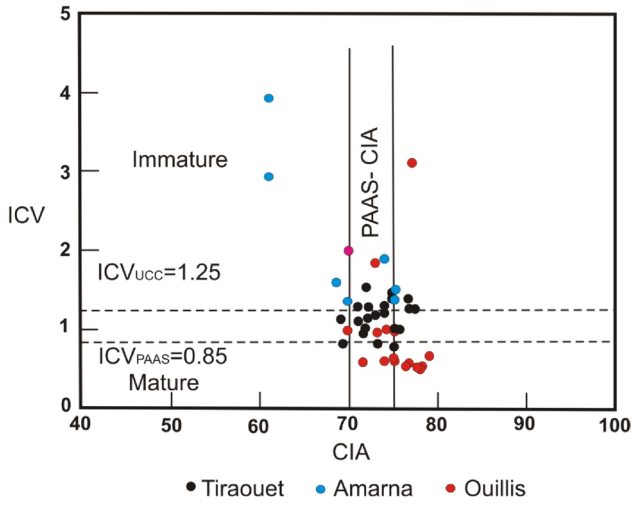

Fig. 9 CIA vs ICV diagram

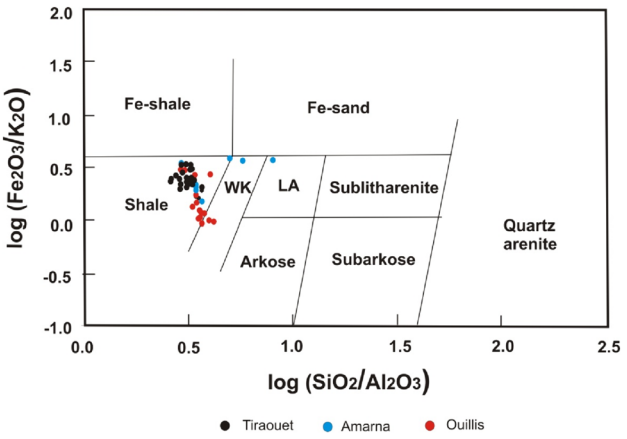

Fig. 11 Plot showing classification of Miocene sediments (from Herron, 1988)

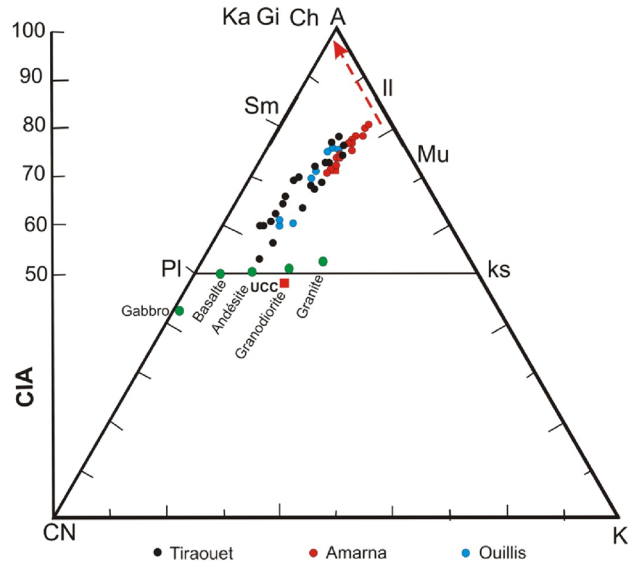

Fig. 10 Ternary A–CN–K diagrams of the studied marl deposits (in molar proportions). Symbols are as follows A: Al_2O_3, CN: $CaO + Na_2O$, K: K_2O, Sm: smectite, Il: illite, Mu: muscovite, Ka: kaolinite, Ch: chlorite, Gi: gibbsite, Pl: plagioclase, Ks: K-feldspar

(Fig. 7). Finally, the highest values are recorded in the lower Messinian marls of the Ouillis section ranging from 77.63 to 92.30 (average 85.38; SD 4.12).

The ICV values of the study sediments are > 1 for the Burdigalian-Langhian sediments of Tiraouet (1.08 to 2.25; average1.72), and lower Tortonian deposits of Amarna (1.98 to 21.64; average 5.58) (Fig. 9).

The ternary molecular A-CN-K plot (A: Al_2O_3, CN: $CaO + Na_2O$, K: K_2O; Nesbitt & Young, 1984) has been applied to the studied Miocene formations (Fig. 10). The chemical weathering trends of the three sections are sub-parallel to the A-CN boundary towards illite composition.

6.3 Chemical proxies for provenance

Few classification schemes have been proposed to classify the siliciclastic sedimentary rocks using major element concentrations (Blatt et al., 1980; Crook, 1974; Pettijohn et al., 1972). Herron (1988) classification, modified from Pettijohn's diagram, is based on the (Na_2O/K_2O) *versus* log (SiO_2/Al_2O_3) diagram. This diagram allows to evaluate the mineral stability (e.g. Descourvieres et al., 2011; Nagarajan et al., 2014; Armstrong-Altrin et al., 2015; Hu et al., 2015; Sahoo et al., 2016). Using the geochemical classification diagram of Herron (1988), most Miocene sediment samples lie in the shale category (Fig. 11).

The SiO_2/Al_2O_3 ratio is a commonly employed indicator of the maturity of sedimentary rocks. Values of this ratio increase during weathering and transport, and recycling is considered as due to an increase in quartz content whereas less resistant components such as feldspar and lithic fragments decrease (Roser et al., 1996).

The SiO_2/Al_2O_3 ratio of Tiraouet (2.46–3.69, average 2.99, SD 0.32) and Ouillis (2.85–4.03, average 3.47, SD 0.30) sedimentary rocks is relatively high. For lower Tortonian deposits of the Amarna section, the SiO_2/Al_2O_3 ratio values vary between 3.47 and 7.84, (average 4.46, SD 0.57).

K_2O/Al_2O_3 ratio ranges between 0.10 and 0.17(average 0.14, SD 0.03) in the Burdigalian-Langhian sediments of Tiraouet section, between 0.14 and 0.19 (average 0.16, SD 0.01), in the Tortonian of Amarna section, and between 0.17 and 0.19 (average 0.18, SD 0.01) in the Messinian of Ouillis section.

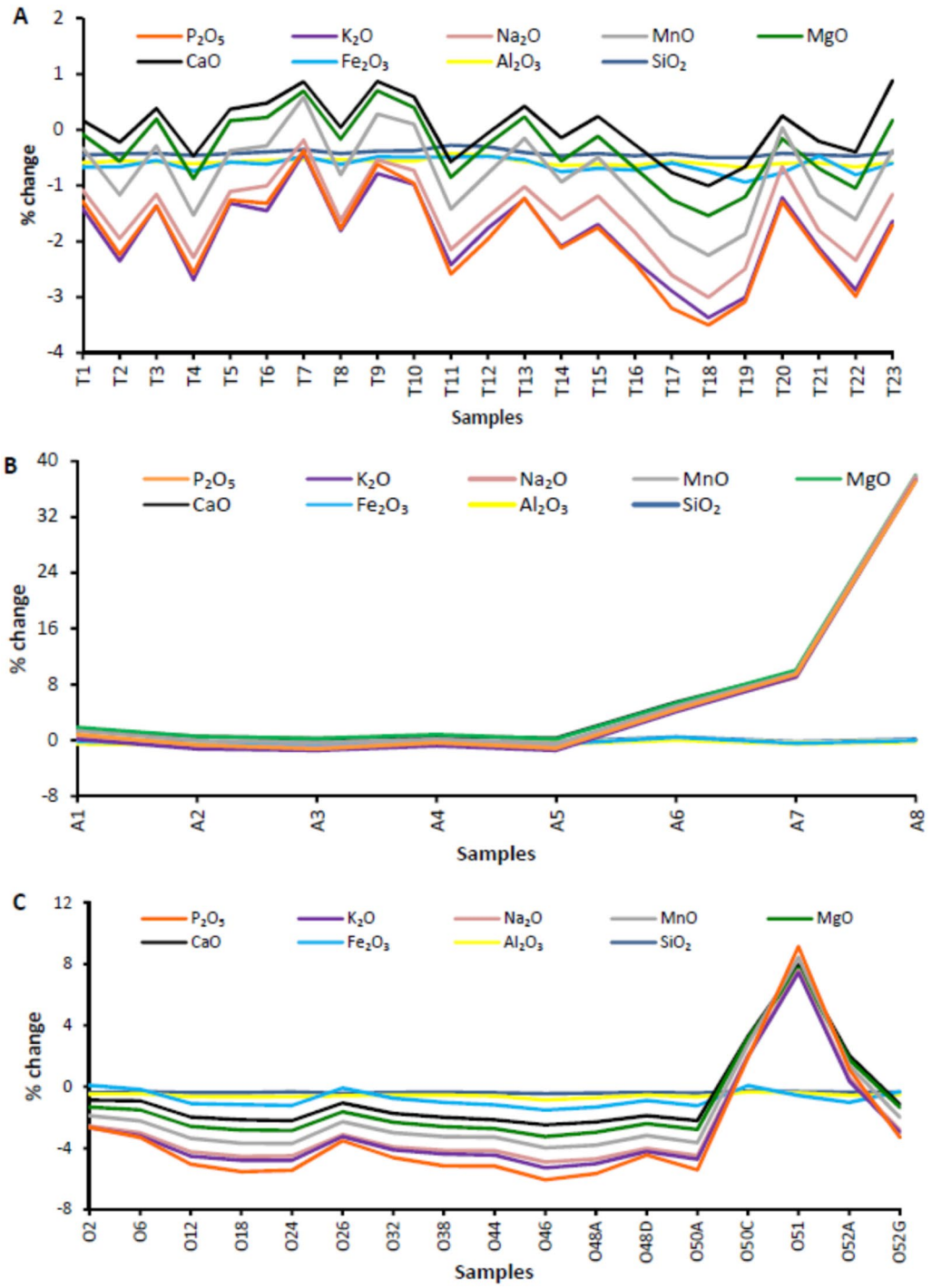

Fig. 12 Binary plot showing major oxides percentage change of **A** Tiraouet, **B** Amarna and **C** Ouillis sections

Al_2O_3/TiO_2 ratios in the study stratigraphic intervals ranges from 19.48 to 21.38 for the Burdigalian-Langhian interval (average 20.24, SD 0.56), 18.23 to 21.65 in the lower Tortonian sediments (average 19.39, SD 0.93), and from 16.83 to 22.31 for lower Messinian (average 19.08, SD 2.13).

6.4 Proxies for chemical mobility and enrichment

The chemical changes accompanying weathering are shown in Figs. 12 and 13. In these diagrams, the contents of each element are plotted against samples. This allows examination

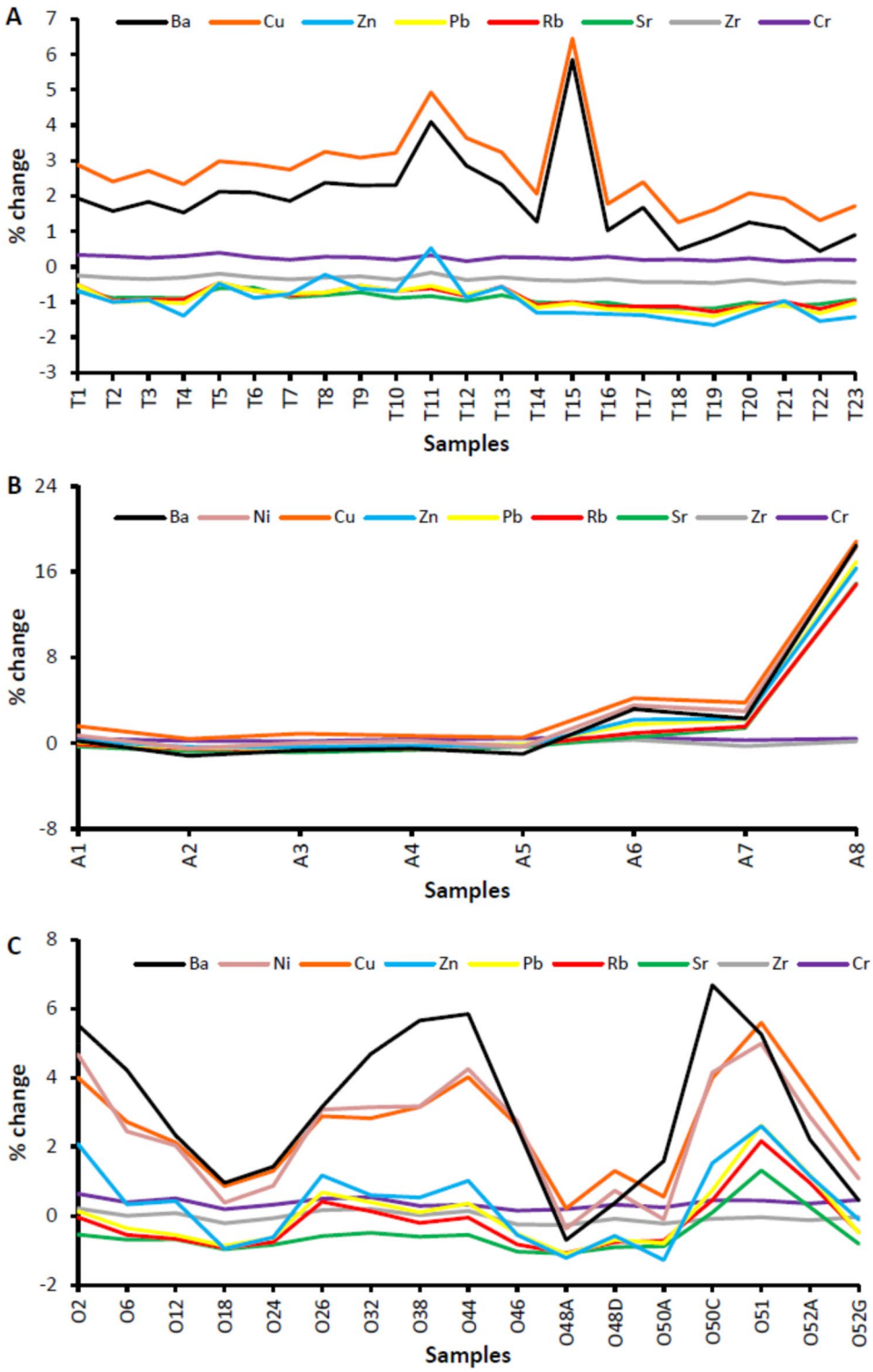

Fig. 13 Binary plot showing trace elements percentage change of **A** Tiraouet, **B** Amarna and **C** Ouillis sections

of relative changes in element concentrations as weathering progressed.

Most of the samples from Tiraouet section (Burdigalian-Langhian) depict strong depletion (compared to UCC) in SiO_2, Al_2O_3, MnO, Na_2O, K_2O, Zr and Sr during the weathering process (Figs. 12 and 13). The UCC contains the maximum concentrations of Fe, Ti, Cr, Zr, and Pb (Hill et al., 2000). All studied sediments show Ba and Cu enrichment (Fig. 13). Samples from the top of Amarna

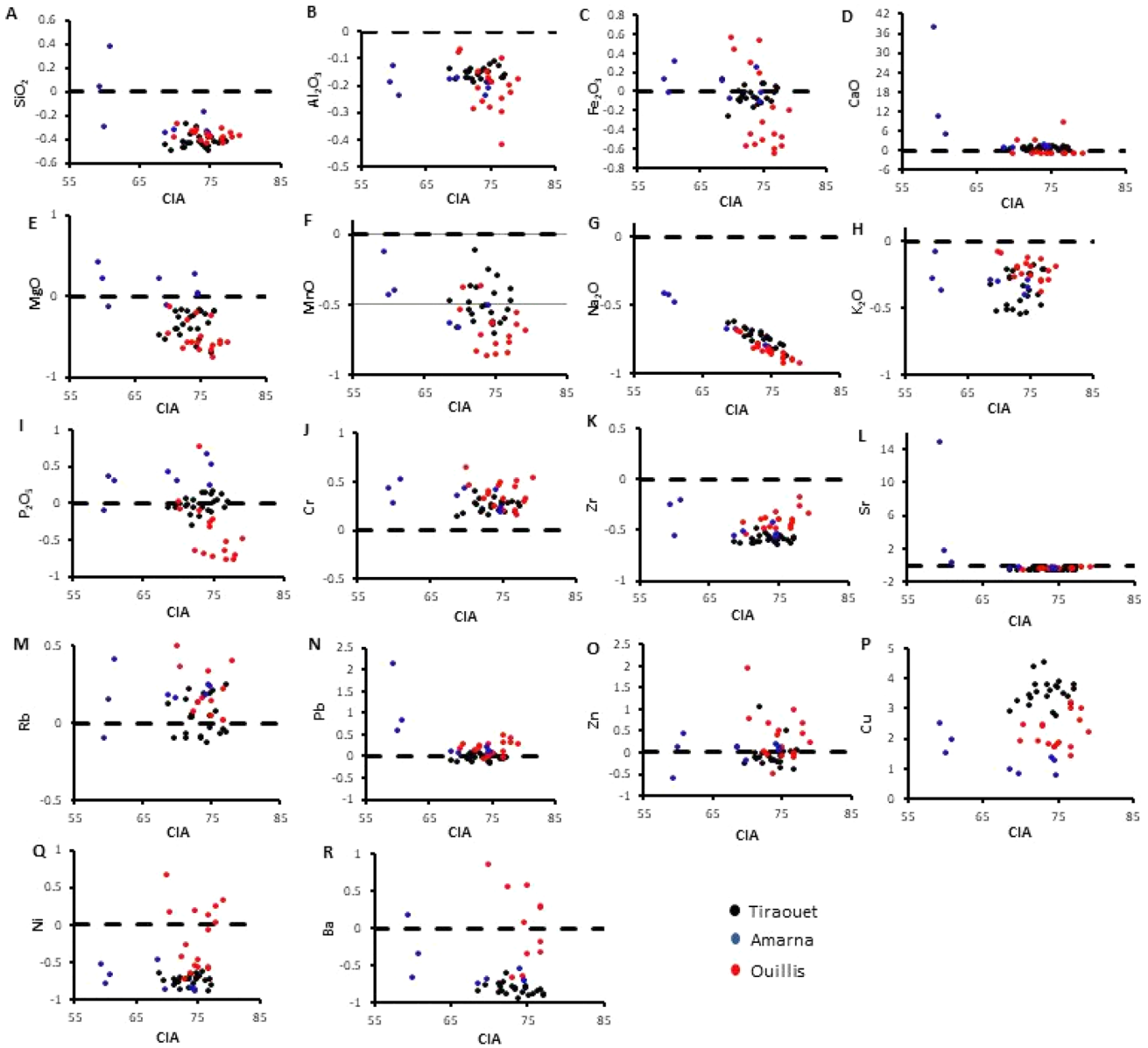

Fig. 14 Chemical mobility during the Chelif sedimentary basin weathering processes. It is calculated in terms of percentage change (normalized with respect to TiO_2 of individual major/trace elements vs. CIA

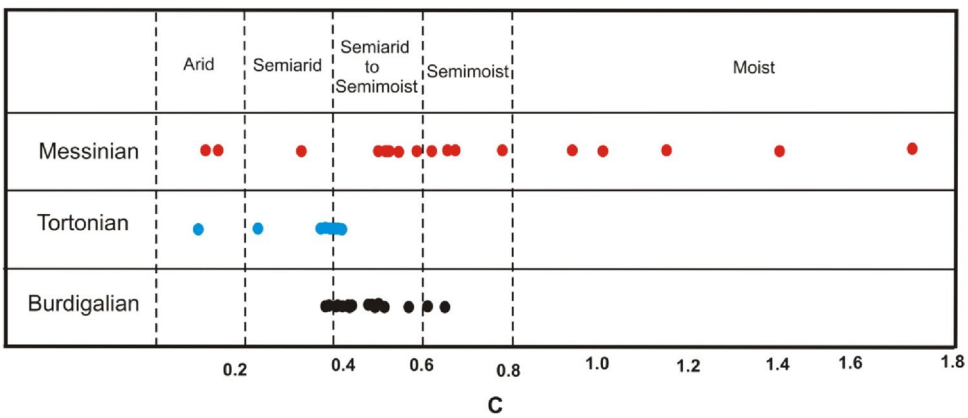

Fig. 15 The C-proxy of Miocene sediments reflecting palaeoclimate

and Ouillis sections (lower Tortonian and lower Messinian respectively) are enriched in Sr.

In order to better examine the geochemical features of the study samples, enrichment factors for major and trace elements (Hassan et al., 1999) relative to UCC (Taylor & McLennan, 1985) are also applied. The enrichment factors were plotted against the CIA values on diagrams (Fig. 14). They can provide a basis for assessing the shift of chemical mobility during progressive chemical weathering in the Lower Chelif Basin. Elements such as Si, Al, Mn, Na, K and Zr show a depletion relative to UCC for the study stratigraphical interval. Depletion of Na is more accentuated than K. Some elements are generally enriched respect to the UCC such as Cr, Cu, Rb, and Zn. The Amarna sediments (lower Tortonian) are generally less depleted in some elements than sediments from Tiraouet and Ouillis sections, such as Si, Fe, Ca, Mg, P, and Pb (Fig. 14).

6.5 Palaeoclimate

From a palaeoclimate point of view, the C-proxy provides valuable insights (Fig. 15). In the Tiraouet section, which represents the Burdigalian-Langhian period, C-proxy range from 0.39 to 0.66, with an average of 0.47 and a standard deviation (SD) of 0.08. On the other hand, in the Amarna section, which represents the lower Tortonian, C-proxy vary from 0.04 to 0.41, averaging at 0.29, with a higher SD of 0.15. Finally, the Ouillis section shows the widest range of C-proxy, spanning from 0.11 to 1.7, with an average of 0.72 and a larger SD of 0.42.

The Sr and Ba are two alkaline-earth metals with similar chemical properties and different behaviors providing valuable insights into palaeosalinity variation (Vosoughi Moradi et al., 2016). The Sr/Ba ratio can be used for determining salinity variation and its corresponding climatic conditions. In general, the Sr/Ba ratio tends to be high in arid conditions compared to humid conditions. This is because in arid environment, there is tipically less rainfall and more evaporation, which can lead to an accumulation of certain elements in water bodies. This higher concentration of Sr relative to Ba results in an elevated Sr/Ba ratio. In contrast, in humid conditions where there is more rainfall and less evaporation, the concentration of Sr and Ba in water bodies tends to be more balanced, leading to a lower Sr/Ba ratio. In our case study, calculated Sr/Ba ratio ranges from 0.44 to 4.51in Tiraouet section, 0.75 to 6.48 in Amarna section, and 0.05 to 1.96 in Ouillis section. There is a moderate negative correlation between C-proxy and Sr/Ba ratio in Tiraouet (r = − 0.44) and Ouillis (r = − 0.48) sections, whereas there is a very strong negative correlation in Amarna section (r = − 0.91) is particularly noteworthy.

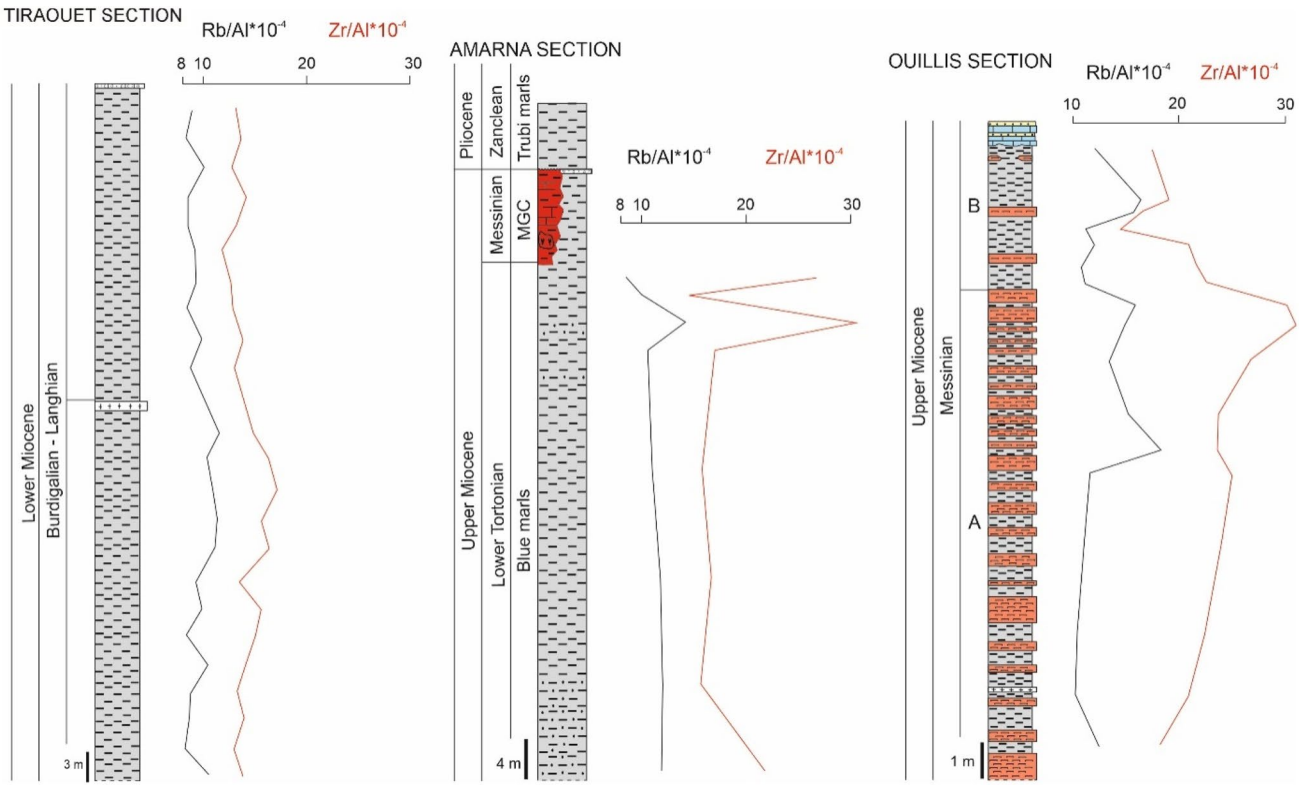

Fig. 16 Stratigraphic distribution of the geochemical detrital proxies for fluvial (Rb/Al) and eolian (Zr/Al) input in the studied sections

Respect to the geochemical detrital proxies, the values of Rb/Al are relatively constant (usually < 15) in the studied stratigraphic interval, but increase in the upper part of the Ouillis section (Fig. 16). The Zr/Al ratio present the highest values in the top of Amarna section and the upper part of the Member A of the Ouillis section (> 20). The sediments of the Tiraouet section present values relatively low (< 20) compared with the upper Miocene sediments (Fig. 16).

7 Discussion

The type of materials forming the Lower Chelif Basin reliefs is characterized by Miocene to Quaternary sediments that unconformably overlie the Mesozoic substratum (Cretaceous schists)(Meghraoui, 1986).

The SiO_2 (46–57.2%) and Al_2O_3 (14.2–20.4%) contents of Miocene sediments do not exhibit large variations in the Burdigalian–Langhian interval unlike the lower Tortonian and lower Messinian where geochemical signatures display abrupt changes. Indeed, in Tortonian, noticeable variations of SiO_2, Al_2O_3 and CaO are noted along the section. Important amounts of SiO_2 exist in its lower part (46.8–55.7%) and decrease to concentrations lower than 29.6%. Similar variations were noted during Messinian of the Ouillis section where very small amounts of CaO (0.08–0.54%), probably due to the absence of calcite, were recorded in the A-member. In the upper two intervals, the decrease in SiO_2 and Al_2O_3 in the upper layers and the increase in CaO indicate weak weathering at the end of the Tortonian and Messinian. This is confirmed by the ICV and SiO_2/Al_2O_3 values that suggest that sediments are immature and enriched in rocks forming minerals.

In a broad context, it is evident that the composition of the sediments suggests a multifaceted origin, likely derived from both magmatic and sedimentary sources. This intricate interplay implies an ongoing recycling process within the geological system. As this recycling unfolds, there is a discernible trend where feldspars, key components in the sedimentary makeup, undergo a gradual depletion. Simultaneously, the relative prevalence of quartz content experiences a progressive increase over an extended period, unveiling a dynamic geological transformation within the sedimentary deposits (Hadji, 2020).

The chemical proxies for weathering and maturity provide valuable insights into environmental processes over time. Within the study area, the Burdigalian–Langhian sediments exhibit CIA values that indicate moderate levels of chemical weathering. This suggests a history of relatively stable environmental conditions with moderate chemical alteration. In contrast, the lower Tortonian sediments stand out with the lowest CIA values indicating a range from weak to moderate chemical weathering. These variations in weathering proxies highlight the dynamic nature of the region environmental history, with distinct phases of weathering intensity (Fig. 7). The PIA values are relatively lower in the lower Tortonian (Amarna section) with a decreasing trend to the top, and the highest values are recorded in the lower Messinian marls (Ouillis section). High values of CIA and PIA suggest that the clastic sediments were the subject of a moderate chemical weathering (Fig. 7).

The ICV values of the study sediments are > 1 for the Burdigalian-Langhian sediments of Tiraouet and lower Tortonian deposits of Amarna (Fig. 9). This suggests that the sediments of the present study are enriched in rock forming minerals such as quartz (5–65%), calcite (5–13%), plagioclase (2–6%), and dolomite (1–6%) (Hadji et al., 2019). In the lower Messinian segment of the Ouillis section, the majority of samples exhibit ICV values below 1 ranging from 0.65–0.98. This indicates an enrichment of clays in the lower part of the section. In its upper part, ICV values are higher (1.1–5.33) indicating the presence of lower content of clay minerals and rock forming minerals (Cox et al., 1995) such as quartz (31–69%), calcite (25–49%), plagioclase (1–4%), orthoclase (1–2%), and gypsum (Hadji, 2020; Hadji et al., 2019).

The degree of chemical weathering is a function of climate and rates of tectonic uplift (Dixon et al., 2012; Fu et al., 2022; Hren et al., 2007; Wronkiewicz & Condie, 1987). The increasing chemical weathering intensity suggests the change of climate towards warm and humid conditions and/or the decrease in tectonic (Jacobson et al., 2003). The Miocene sediments show CIA values > 50, and reflect weak to moderate weathering conditions in the source area of the sediments. These results are supported by PIA and ICV values. Low CIA and PIA, as well as high ICV (> 1) values are observed in the upper part of Amarna section (lower Tortonian) and indicate the near absence of chemical weathering and might reflect arid climate conditions (Fig. 16).

The application of the A-CN-K ternary molecular plot (Babechuk et al., 2014; Fedo & Babechuk, 2023; Nesbitt & Young, 1984, 1989; Patel et al., 2022) to the analyzed sediments (Fig. 10) demonstrates that the chemical weathering trends align closely to the A-CN boundary, indicating a shift towards illite composition. This observation confirms the preferential removal of Ca and Na over K from feldspars (Nesbitt & Young, 1984).

The geochemical proxy for provenance, SiO_2/Al_2O_3 ratio is a commonly used index of sedimentary maturation (Murkute, 2023; Roser et al., 1996; Sonowal et al., 2022). This ratio tends to rise as sediments undergo weathering and transportation. The increase is attributed to the greater abundance of durable framework quartz relative to less

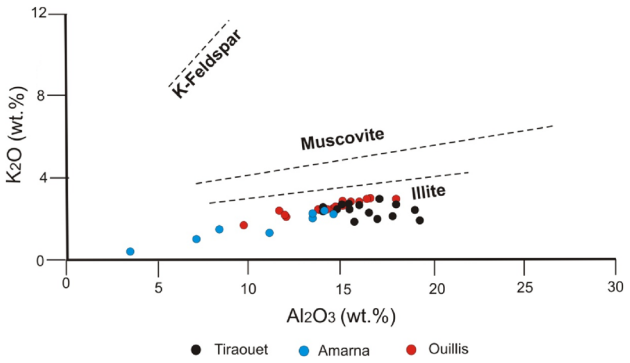

Fig. 17 K_2O versus Al_2O_3 diagram

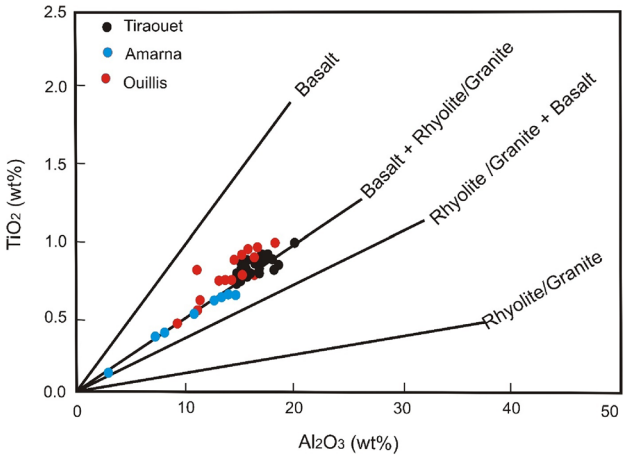

Fig. 18 Plots of TiO_2 versus Al_2O_3 on the diagram for Miocene sediments (from Amajor, 1987)

resilient components like feldspar and lithic fragments, suggesting recycling process (Roser et al., 1996). SiO_2/Al_2O_3 values > 5–6 in sedimentary rocks are indicative of sedimentary maturation (Roser et al., 1996). This ratio typically decreases in parallel to grain size or textural maturity within a given size range. This is owing to the relative enrichment of Al-rich phyllosilicates at the expense of Si-rich phases in fine-grained materials (Weltje & Eynatten, 2004).The SiO_2/Al_2O_3 ratio of Tiraouet (2.46–3.69) and Ouillis (2.85–4.03) are indicative of low-maturity chemical of sedimentary rocks compared with lower Tortonian deposits of the Amarna section where the SiO_2/Al_2O_3 ratio values are higher (3.47–7.84) and maturity was moderate.

In the examined stratigraphic intervals of the Lower Chelif Basin, K_2O/Al_2O_3 ratios range between 0.10 and 0.19. These values fall within the range proposed by Cox et al. (1995) (values < 0.4), signifying a dominance of clay minerals over those rich in K. This indicates that the original source rocks of sediment likely contained minimal alkali feldspar relative to other minerals. On the K_2O *versus* Al_2O_3 diagram (Fig. 17), all samples of the studied sections are located close to the illite line and suggest that the major Al_2O_3 and K_2O bearing minerals are illite that probably originate from K-feldspar decomposition.

The Al_2O_3/TiO_2 values ranging from 16.83 to 22.31 suggest that intermediate to felsic rocks would have acted as source rocks for the shale samples of the present study. Amajor (1987) proposed the TiO_2 vs Al_2O_3 binary plot as a provenance indicator. The application of this plot on Miocene sediments of Lower Chelif Basin (Fig. 18) indicates that all samples fall along the basalt + rhyolite/granite line. This confirms that these sediments are derived from mixed source sediments, the composition of which ranges from mafic to felsic source rocks.

Concerning to the proxies for chemical mobility, the enrichment factors indicate a chemical mobility during the chemical weathering in the Lower Chelif Basin favoured depletion of Si, Al, Mn, Na, K and Zr respect to UCC and enrichment for Cr, Cu, Rb and Zn. Depletion of Na is more accentuated than K, suggesting enhanced alteration of plagioclase as compared to K-feldspar. The lower Tortonian sediments of Amarna section are generally less depleted in Si, Fe, Ca, Mg, P, and Pb than sediments from Tiraouett and Ouillis sections (Fig. 16).

The distribution of C-proxy of the three stratigraphic intervals in the Lower Chelif Basin (Fig. 15) presents variable values that range between 0.39 and 0.66 for Tiraouet section (Burdigalian – Langhian), 0.04 to 0.41 for Amarna section (lower Tortonian), and 0.11 to 1.7 for Ouillis section (lower Messinian). Therefore, the C-value, used as a geochemical proxy for palaeoclimate (according to Zhao et al., 2007; Cao et al., 2015; Vosoughi Moradi et al., 2016), suggests a generally semi-arid to semi-moist climate during the Burdigalian–Langhian and arid to semiarid one during the early Tortonian in the Lower Chelif Basin (Fig. 17). Conditions during the early Messinian were variable according to C-proxy from Ouillis section but mainly related to relatively humid conditions. The fluvial detrital proxy Rb/Al present the highest values in the Ouillis section confirming enhanced fluvial input of sediment probably related to more humid conditions. The eolian detrital proxy Zr/Al presents the highest values in the top of the Amarna section and the upper part of the Member A of the Ouillis section indicating punctual increased eolian input of sediment probably related to arid conditions.

The Sr/Ba ratio increase with the salinity of water masses (Cao et al., 2015; Meng et al., 2012) and high Sr/Ba ratio indicates a high salinity degree related to hot arid climate conditions and low Sr/Ba indicates low salinity degree potentially related to humid climate (Vosoughi Moradi et al., 2016). The Sr/Ba values of the studied

sediments evidence a palaeoenvironment with variable salinity during the Miocene in the Lower Chelif Basin, with relatively higher salinity during the early Tortonian (highest values in the Amarna section).

Low Sr/Ba ratio values suggest conditions that are likely less arid and possibly more humid for Tiraouet (Burdigalian–Langhian) and Ouillis (lower Messinian) sections. This could indicate environments with more consistent rainfall and lower evaporation rates and probably some seasonal variations, experiencing wet and dry seasons.High Sr/Ba values of Amarna section suggest environments that have experienced significant evaporation and concentration of elements during the lower Tortonian, consistent with semi-arid to arid conditions.

A moderate negative correlations between C-proxy and Sr/Ba ratio in Tiraouet ($r = -0.44$) and Ouillis ($r = -0.48$) suggest that certain palaeoclimatic conditions were associated with specific elemental compositions. The very strong negative correlation in Amarna section ($r = -0.91$) is particularly noteworthy and indicates an extremely close relationship between the palaeoclimate conditions represented by the C-proxy and the Sr/Ba ratio. This suggests that the environmental signals recorded by these proxies are tightly linked, possibly reflecting a more sensitive response to climate variations in this specific location during the early Tortonian.

8 Conclusions

The inorganic geochemistry of Miocene sediments from the Lower Chelif Basin provide us valuable insights into palaeoenvironmental conditions and processes that shaped this region during the Miocene period. The major oxide and trace element compositions show distinct variations across the stratigraphic intervals. The lower Miocene sediments of the Tiraouet section exhibit relatively stable major oxide contents indicating a consistent source material but show a strong depletion compared to UCC in SiO_2, Al_2O_3, MnO, Na_2O, K_2O, Zr and Sr related to weathering process. The trace element concentrations, particularly Sr, Cu and Ba, provide additional insights into the geochemical signature of these sediments. In contrast, the Tortonian sediments in the Amarna section display notable variations in major oxides contents, suggesting changes in source material and weathering conditions. The lower Messinian sediments of the Ouillis section present unique major oxide composition, notably low CaO, reflecting distinct sedimentary processes and environmental conditions.

Chemical proxies for weathering and maturity, including CIA, PIA, and ICV values provide further context on the degree of chemical alteration and sediment maturity. The results suggest varying levels of weathering intensity across different stratigraphic intervals, indicating shifts in climatic and tectonic conditions. ICV values suggest that during Burdigalian–Langhian and Tortonian, sediments were enriched in rocks forming minerals, and the Al_2O_3 versus K_2O diagram, of the three stratigraphic intervals are close to the illite line and suggest that the major Al_2O_3 and K_2O bearing mineral is illite, probably originating from K-feldspar decomposition.

Palaeoclimate proxies, including C-proxy and Sr/Ba ratios, offer important information about past climate conditions. The results indicate a range of palaeoclimates, from semi-arid to semi-moist conditions during the Burdigalian-Langhian, and from arid to semi-arid conditions during the Tortonian.

Acknowledgements Financial support through the RNM-200 Research Group (Junta de Andalucía, Spain) and the project PID2019-104625RB-100 (Spanish Government) are gratefully acknowledged. We thank the Associated Editor Ana Bernabeu and two anonymous reviewers for their comments and suggestions.

Data availability The data is available from the Geology Laboratory of the University of Tlemcen.

Declarations

Conflict of interest The author declares no competing interests.

References

Aïfa, T., Feinberg, H., Derder, M. M., & Merabet, N. (1992). Rotations paléomagnétiques récentes dans le bassin du Chéliff (Algérie). *Comptes Rendus De L'académie Des Sciences, 314*, 915–922.

Aïfa, T., Feinberg, H., Derder, M. M., & Merabet, N. (2003). Contraintes magnétostratigraphiques concernant la durée de l'interruption des communications marines en Méditerrannée occidentale pendant le Messinien supérieur. *Geodiversitas, 25*, 617–631.

Amajor, L. C. (1987). Major and trace elements geochemistry of Albin and Turonian shales from the Southern Benue trough, Nigeria. *Journal of African Earth Sciences, 6*, 633–641.

Ameur-Chehbeur, A. (1988). Biochronologie des formations continentales du Néogène et du Quaternaire de l'Algérie. Contribution des micromammifères. *PhD Thesis*, Université d'Oran, 432 p.

Arab, M. R., Roure, F., Zazoun, R. S., Mahdjoub, Y., & Badji, R. (2015). Source rocks and related petroleum systems of the Chelif Basin, (western Tellian domain, north Algeria). *Marine and Petroleum Geology, 64*, 363–385.

Armstrong-Altrin, J. S., Machain-Castillo, M. L., Rosales-Hoz, L., Carranza-Edwards, A., Sanchez-Cabeza, J. A., & Ruíz-Fernández, A. C. (2015). Provenance and depositional history of continental slope sediments in the southwestern Gulf of Mexico unraveled by geochemical analysis. *Continental Shelf Research, 95*, 15–26.

Atif, K. F. T., Bessedik, M., Belkebir, L., Mansour, B., & Saint Martin, J. P. (2008). Le passage Mio-Pliocène dans le bassin du Bas Chélif (Algérie). *Biostratigraphie Et Paléoenvironnements. Geodiversitas, 30*, 97–116.

Babechuk, M. G., Widdowson, M., & Kamber, B. S. (2014). Quantifying chemical weathering intensity and trace element release from two contrasting basalt profiles, Deccan Traps, India. *Chemical Geology, 363*, 56–75.

Belhadji, A., Belkebir, L., Saint Martin, J. P., Mansour, B., Bessedik, M., & Conesa, G. (2008). Apports des foraminifères planctoniques à la biostratigraphie du Miocène supérieur et du Pliocène

de Djebel Diss (bassin du Chélif, Algérie). *Geodiversitas, 30*, 79–96.

Belkebir, L. (1986). Le Néogène de la bordure nord - occidentale du massif de Dahra (Algérie). Biostratigraphie, Paléoécologie, Paléogéographie. *PhD Thesis*, Université de Provence

Belkebir, L., Bessedik, M., Ameur-Chehbour, A., & Anglada, R. (1996). Le Miocène des bassins nord occidentaux d'Algérie : Biostratigraphie et eustatisme, in Géologie de l'Afrique et de l'Atlantique Sud, actes Colloques Angers 1994. *Elf Aquitaine Éditions, 16*, 553–561.

Belkebir, L., Bessedik, M., & Mansour, B. (2002). Le Miocène supérieur du Bassin du Bas Chélif : Attribution biostratigraphique à partir des foraminifères planctoniques. *Mémoires Du Service Géologique De L'algérie, 11*, 187–194.

Bessedik, M., Belkebir, L., & Mansour, B. (2002). Révision du Miocène inférieur (au sens des anciens auteurs) des dépôts du bassin du bas Chelif (Oran, Algérie). Conséquences biostratigraphiques et géodynamiques. *Mémoires Du Service Géologique National De L'algérie, 11*, 167–186.

Blatt, H., Middleton, G., & Murray, R. (1980). *Origin of sedimentary rocks*. Englewood dins: Prentice-Hall.

Cao, H., Guo, W., Shan, X., Ma, L., & Sun, P. (2015). Paleolimnological environments and organic accumulation of the Nenjiang Formation in the southeastern Songliao Basin. *China, Oil Shale, 32*, 5–24.

Chester, R., Baxter, G. B., Behairy, A. K. A., Connor, K., Cross, D., Elderfield, H., & Padghamm, R. C. (1977). Soil-sized eolian dusts from the lower troposphere of the eastern Mediterranean Sea. *Marine Geology, 24*, 201–217.

Chesworth, W., Dejou, J., & Larroque, P. (1981). The weathering of basalts and relative mobilities of the major elements at Belbex, France. *Geochemical Et Cosmochimica Acta, 45*, 1235–1243.

Cox, R., Lower, D. R., & Cullers, R. L. (1995). The influence of sediment recycling and basement composition on evolution of mud rock chemistry in the southwestern United States. *Geochemical Et Cosmochimica Acta, 59*, 2919–2940.

Crook, K.A.W. (1974). Lithogenesis and geotectonics: the significance of compositional variation in flysch arenites (graywackes). In: Dott Jr., R.H., Shaver, R.H. (Eds.), Modern and Ancient Geosynclinal Sedimentation, *Special Publications-SEPM*, 19, 304–310.

Descourvieres, C., Douglas, G., Leyland, L., Hartog, N., & Prommer, H. (2011). Geochemical reconstruction of the provenance, weathering and deposition of detrital-dominated sediments in the Perth Basin: The Cretaceous Leederville Formation, south-west Australia. *Sedimentary Geology, 236*, 62–76.

Dixon, J. L., Hartshorn, A. S., Heimsath, A. M., DiBiase, R. A., & Whipple, K. X. (2012). Chemical weathering response to tectonic forcing: A soils perspective from the San Gabriel Mountains, California. *Earth and Planetary Science Letters, 323–324*, 40–49.

Fedo, C. M., & Babechuk, M. G. (2023). Petrogenesis of siliciclastic sediments and sedimentary rocks explored in three-dimensional Al_2O_3–CaO*+Na_2O–K_2O–FeO+MgO (A–CN–K–FM) compositional space. *Canadian Journal of Earth Sciences*. https://doi.org/10.1139/cjes-2022-005

Fedo, C. M., Nesbitt, H. W., & Young, G. M. (1995). Unraveling the effects of K-metasomatism in sedimentary rocks and paleosols with implications for palaeoweathering conditions and provenance. *Geology, 23*, 921–924.

Fu, H., Jian, X., Liang, H., Zhang, W., Shen, X., & Wang, L. (2022). Tectonic and climatic forcing of chemical weathering intensity in the northeastern Tibetan Plateau since the middle Miocene. *CATENA, 208*, 105785.

Hadji, F. (2020). Les marnes du Miocene de l'Oranie: Caractérisation minéralogique et géochimique. *PhD Thesis,* Université de Tlemcen

Hadji, F., Marok, A., & Mokhtar Samet, A. (2019). Miocene sediment mineralogy of the lower Chelif basin (NW Algeria): Implications for weathering and provenance. *Turkish Journal of Earth Sciences, 28*, 85–102.

Harnois, L. (1988). The CIW index: A new Chemical Index of weathering. *Sedimentary Geology, 55*, 319–322.

Hassan, S., Ishiga, H., Roser, B. P., Dozen, K., & Naka, T. (1999). Geochemistry of Permian–Triassic shales in the Salt Range, Pakistan: Implications for provenance and tectonism at the Gondwana margin. *Chemical Geology, 158*, 293–314.

Hayashi, K. I., Fujisawa, H., Holland, H. D., & Ohomoto, H. (1997). Geochemistry of ~1.9 Ga sedimentary rocks from northern Labrador, Canada. *Geochemical Et Cosmochimica Acta, 61*, 4115–4137.

Herron, M. M. (1988). Geochemical classification of terrigenous sands and shales from core or log data. *Journal of Sedimentary Petrology, 58*, 820–829.

Hill, I. G., Worden, R. H., & Meighan, I. G. (2000). Geochemical evolution of a palaeolaterite: The Interbasaltic Formation, Northern Ireland. *Chemical Geology, 166*, 65–84.

Hren, T. M., Hilley, G. E., & Chamberlain, C. P. (2007). The relationship between tectonic uplift and chemical weathering rates in the Washington Cascades: Field measurements and model predictions. *American Journal of Sciences, 307*, 1041–1063.

Hu, J., Li, Q., Fang, N., Yang, J., & Ge, D. (2015). Geochemistry characteristics of the Low Permian sedimentary rocks from central uplift zone, Qiangtang Basin, Tibet: Insights into source-area weathering, provenance, recycling, and tectonic setting. *Arabian Journal of Geosciences, 8*, 5373–5388.

Jacobson, A. D., Blum, J. D., Chamberlain, C. P., Craw, D., & Koons, P. O. (2003). Climatic and tectonic controls on chemical weathering in the New Zealand Southern Alps. *Geochimica Et Cosmochimica Acta, 67*, 29–46.

Jian, C., Ming, W., Yan, C., Kai, H., Lizeng, B., Longgang, W., & Ying, Z. (2012). Trace and rare earth element geochemistry of Jurassic mudstones in the northern Qaidam Basin, northwest China. *Chemie Der Erde, 72*, 245–252.

Liu, Z., Zhao, Y., Colin, C., Siringan, F. P., & Wu, Q. (2009). Chemical weathering in Luzon, Philippines from clay mineralogy and major-element geochemistry of river sediments. *Applied Geochemistry, 24*, 2195–2205.

Mansour, B., Bessedik, M., Saint Martin, J.-P., & Belkebir, L. (2008). Signification paléoécologie des assemblages de diatomées du Messinien du Dahra sud-occidental (bassin du Chelif, Algérie nord-occidental). *Geodiversitas, 30*, 117–139.

Maslov, A. V., Krupenin, M. T., & Gareev, E. Z. (2003). Lithological, lithochemical, and geochemical indicators of paleoclimate: Evidence from Riphean of the Southern Urals. *Lithology and Mineral Resources, 38*, 427–446.

McLennan, S.M. (2001). Relationships between the trace element composition of sedimentary rocks and upper continental crust. *Geochemistry, Geophysics, Geosystems, 2*, 2000GC000109.

Meghraoui, M. (1982). Étude néotectonique de la région nord-ouest d'El-Asnam: relation avec le séisme du 10 octobre 1980. *Thesis 3ème cycle*, Université de Paris VII.

Meghraoui, M. (1986). Seismotectonics of the Lower Cheleff basin: Structural Background of the El Asnam (Algeria) earthquake. *Tectonics, 6*, 809–836.

Meng, Q. T., Liu, Z. J., Bruch, A. A., Liu, R., & Hu, F. (2012). Palaeoclimatic 438 evolution during the Eocene and its influence on oil shale mineralization, Fushun Basin, China. *Journal of Asia Earth Sciences, 45*, 95–105.

Middleburg, J. J., van der Weijden, C. H., & Woittiez, J. R. W. (1988). Chemical processes affecting the mobilities of major, minor and trace elements during the weathering of granitic rocks. *Chemical Geology, 68*, 253–273.

Mokhtar Samet, A., Marok, A., Reolid, M. & Kamikuri, S.I. (2021). Les radiolaires messiniens du Dahra (Bassin du Bas Chélif, Algérie): systématique et intérêt biostratigraphique. *Annales de Paléontologie, 107*, 102520.https://doi.org/10.1016/j.annpal.2021.102520.

Mokhtar Samet, A., Reolid, M., Marok, A., & Kamikuri, S. I. (2022). Environmental conditions during the deposition of the diatomite–organic-rich marl alternation of the lower Messinian of the Lower Chelif Basin (Algeria) interpreted from microfossil assemblages and geochemistry. *Journal of African Earth Sciences, 190*, 104521. https://doi.org/10.1016/j.jafrearsci.2022.104521

Moosavirad, S. M., Janardhanab, M. R., Sethumadhav, M. S., Moghadam, M. R., & Shankara, M. (2011). Geochemistry of Lower Jurassic shales of the Shemshak Formation, Kerman Province, Central Iran: Provenance, source weathering and tectonic setting. *Chemie Der Erde, 7*, 279–288.

Murkute, Y. A. (2023). Petrography and geochemistry of Sullavai Sandstones of Kanpa-Tempa, Chandrapur District, Maharashtra, India. *Journal of the Geological Society of India, 99*, 1225–1233.

Nagarajan, R., Roy, P. D., Jonathan, M. P., Lozano, R., Kessler, F. L., & Prasanna, M. V. (2014). Geochemistry of Neogene sedimentary rocks from Borneo Basin, East Malaysia: Paleo-weathering, provenance and tectonic setting. *Chemie Der Erde-Geochemistry, 74*, 139–146.

Nesbitt, H. W. (1979). Mobility and fractionation of rate earth elements during weathering of a granodiorite. *Nature, 279*, 206–210.

Nesbitt, H. W., Marcovics, G., & Price, R. C. (1980). Chemical processes affecting alkalis and alkaline earths during continental weathering. *Geochimica Et Cosmochimica Acta, 44*, 1659–1666.

Nesbitt, H. W., & Young, G. M. (1982). Early Proterozoic climates and plate motions inferred from major element chemistry of lutites. *Nature, 299*, 715–717.

Nesbitt, H. W., & Young, G. M. (1984). Prediction of some weathering trends of plutonic and volcanic rocks based on thermodynamic and kinetic considerations. *Geochimica Et Cosmochimica Acta, 48*, 1523–1534.

Nesbitt, H. W., & Young, G. M. (1989). Formation and diagenesis of weathering profiles. *Journal of Geology, 97*, 129–147.

Neurdin-Trescartes, J. (1992). Le remplissage sédimentaire du bassin Néogène du Chelif, modèle de référence de bassins intramontagneux. *PhD Thesis,* Université de Pau.

Neurdin-Trescartes, J. (1995). Paléogéographie du bassin de Chélif (Algérie) au Miocène. Causes et Conséquences. *Géologie Méditerranéenne, XXII, 2*, 61–71.

Parker, A. (1970). An index of weathering for silicate rocks. *Geological Magazine, 107*, 501–504.

Patel, A., Raj, R., & Tripathi, J. K. (2022). Geochemical trends and rare Earth elements' behaviour in the recently exposed weathering profiles of the Deccan Basalts from Central India. *Journal of the Geological Society of India, 98*, 1653–1660.

Pettijohn, F. J., Potter, P. E., & Siever, R. (1972). *Sand and sandstone*. Springer.

Pye, K. (1987). *Aeolian dust and dust deposits* (p. 334). Academic Press.

Rodríguez-Tovar, F. J., & Reolid, M. (2013). Environmental conditions during the Toarcian Oceanic Anoxic Event (T-OAE) in the westernmost Tethys: Influence of the regional context on a global phenomenon. *Bulletin of Geosciences, 88*, 697–712.

Roser, B. P., Cooper, R. A., Nathan, S., & Tulloch, A. J. (1996). Reconnaissance sandstone geochemistry, provenance, and tectonic setting of the lower Paleozoic terranes of the West Coast and Nelson, New Zealand. *New Zealand Journal of Geology and Geophysics, 39*, 1–16.

Rouchy, J. M. (1982). La genèse des évaporites messiniennes de Méditerranée. *Mémoires Du Muséum National D'histoire Naturelle, 50*, 1–265.

Rouchy, J. M., Caruso, A., Pierre, C., Blanc-Valleron, M. M., & Bassetti, M. A. (2007). The end of the Messinian salinity crisis: Evidences from the Chelif Basin (Algeria). *Palaeogeography, Palaeoclimatology, Palaeoecology, 254*, 386–417.

Rudnick, R. L., & Gao, S. (2003). Composition of the continental crust. *Treatise of Geochemistry, 3*, 1–64.

Sahoo, P. K., Felix Guimarães, J. T., Martins Souza-Filho, P. W., Sousa da Silva, M., Maurity, C. W., Powell, M. A., Rodrigues, T. M., Fonseca da Silva, D., Mardegan, S. F., Furtini Neto, A. E., & Dall'Agnol, R. (2016). Geochemistry of upland lacustrine sediments from Serra dos Carajás, Southeastern Amazon, Brazil: Implications for catchment weathering, provenance, and sedimentary processes. *Journal of South American Earth Sciences, 72*, 178–190.

Saint-Martin, J. P. (1990). Les formations récifale coralliennes du Miocène supérieur d'Algérie et du Maroc. Aspects paléoécologiques et paléogéographiques. *Mémoires Du Muséum National D'histoire Naturelle, 56*, 1–366.

Singh, M., Sharma, M., & Tobschall, H. J. (2005). Weathering of the Ganga alluvial plain, northern India: Implications from fluvial geochemistry of the Gomati River. *Applied Geochemistry, 20*, 1–21.

Song, C., Hu, S., Han, W., Zhang, T., Fang, X., Gao, J., & Wu, F. (2014). Middle Miocene to earliest Pliocene sedimentological and geochemical records of climate change in the western Qaidam Basin on the NE Tibetan Plateau. *Palaeogeography, Palaeoclimatology, Palaeoecology, 395*, 67–76.

Sonowal, P., Khan, T., Gogoi, M., Kumar, T. S., Walling, T., & Phukan, S. (2022). Petrography and geochemistry of sandstones of Eocene Kopili Formation, Shillong Plateau: Implications on paleo-weathering, provenance and tectonic setting. *Journalof Geological Societyof India, 98*, 219–231.

Taylor, S. R., & McLennan, S. M. (1985). *Crust: Its Composition and Evolution*. Blackwell Scientific Publications.

Thomas, H. (1985). Géodynamique d'un bassin intramontagneux. Le bassin du Bas Chelif occidental durant le Mio-Plio-Quaternaire. *PhD Thesis*, Université de Pau et Pays de l'Adour.

Vosoughi Moradi, A., Sarı, A., & Akkaya, P. (2016). Geochemistry of the Miocene oil shale (Hançili Formation) in the Çankırı-Çorum Basin, Central Turkey: Implications for Paleoclimate conditions, source-area weathering, provenance and tectonic setting. *Sedimentary Geology, 341*, 289–303.

Weltje, G. J., & Von Eynatten, H. (2004). Quantitative provenance analysis of sediments: Review and outlook. *Sedimentary Geology, 171*, 1–11.

Wildi, W. (1983). La chaine tello-rifaine (Algérie, Maroc, Tunisie): Structure, stratigraphie et évolution du Trias au Miocène. *Revue De Géographie Physique Et De Géologie Dynamique, 24*, 201–297.

Wronkiewicz, D. J., & Condie, K. C. (1987). Geochemistry of Archean Shales from the Witwatersrand Super group, South Africa: Source-Area Weathering and Provenance. *Geochimimica Et Cosmochimica Acta, 51*, 2401–2416.

Zhao, Z. Y., Zhao, J. H., Wang, H. J., Liao, J. D., & Liu, C. M. (2007). Distribution characteristics and applications of trace elements in Junggar Basin. *Natural Gas Exploration and Development, 30*, 30–33.